Effects of Additives on Catalytic Arene C–H Activation: Study of Rh Catalysts Supported by Bis-phosphine Pincer Ligands

Fanji Kong, Shunyan Gu, Chang Liu, Diane A. Dickie, Sen Zhang and T. Brent Gunnoe*

Department of Chemistry, University of Virginia, Charlottesville, Virginia 22904, United States

*Correspondence to: tbg7h@virginia.edu

Abstract

Hydrogen–deuterium exchange (H/D exchange) is a commonly used method for studying catalytic activation of C–H(D) bonds by transition metal complexes. In this study, a series of Lewis acid additives were studied for H/D exchange of toluene-d_8 with acetic acid (HOAc) using (^{R}PNP)Rh(X) complexes (R = phosphine substituents including cyclohexyl, isopropyl and *tert*-butyl; X = trifluoroacetate or acetate) as the pre-catalysts. $Cu(OAc)_2$ and AgOAc additives were found to benefit Rh-mediated C–H(D) activation of toluene with *meta-para* selectivity by facilitating the conversion to active (^{R}PNP)Rh species and stabilizing the Rh catalysts from decomposition to inactive Rh(s). In contrast, non-oxidizing Lewis acid additives, such as $B(OMe)_3$ or NaOAc, were not effective at facilitating Rh-catalyzed toluene C–H activation. The complexes (^{R}PNP)$Rh^{III}(H)(X)_2$ and [(^{R}PNP)Rh^{I}(CO)][X] (X = TFA or OAc) were found to be intermediates of the catalytic the H/D exchange.

Introduction

Catalytic functionalization of carbon–hydrogen (C–H) bonds offers potential applications including the conversion of hydrocarbons to higher value commodity chemicals as well as the development of new methodologies for producing fine chemicals.[1-21] However, challenges remain in the field of selective transformation of C–H bonds to functionalized C–C or C–X (X = heteroatom or halogen) bonds.[22-29] For example, the high bond dissociation energies and the non-polar nature of C–H bonds of hydrocarbons make both heterolytic and homolytic C–H bond cleavage challenging.[22-24] Discrete C–H activation reactions are often thermodynamically disfavored, which can negatively impact the kinetics of catalytic processes that are overall thermodynamically favorable.[25,30] Also, the C–H bonds of the functionalized products are often weaker than those of starting reagents, and, hence, functionalized products are often more reactive than starting hydrocarbons.[25,27-28,31]

Ligated transition metal catalysts provide the potential to adjust reactivity and selectivity due to their tunable steric and electronic properties and are now used for diverse selective C–H functionalization reactions.[5-7,12,23,27-29,32-41] In general, transition metal-mediated C–H functionalization processes can be divided into two key overall steps. The initial step is the C–H activation transformation, which involves a C–H bond cleavage reaction that leads to the formation of an intermediate containing a M–C bond.[42] The second step involves conversion of the M–C (C = ligand that results from the C–H activation step) intermediate to a functionalized product by subsequent reaction(s). In order to achieve efficient and selective C–H functionalization, different strategies have been used to accelerate the C–H activation step. These include the incorporation of directing groups in the substrate that facilitate coordination to the catalyst[37,43-50] and the use of co-catalysts to accelerate C–H activation.[51-52]

Recently, examples of Lewis acid facilitated C–H activation and functionalization have been reported (Scheme 1).[53-58] In 2012, the Huang group reported the use of $ZnCl_2$ with pivalic acid (HOPiv) to increase the yield of Pd-catalyzed benzisoxazolone synthesis.[53] Later, Sunoj and coworkers demonstrated the role of $ZnCl_2$ and pivalic acid using density functional theory (DFT) calculations.[54] They proposed that the Lewis acidic Zn^{II} serves to bond with Pd and stabilize the C_{aryl}–N bond forming transition state through a Pd–Zn heterobimetallic interaction.[54] Novak and coworkers reported that the presence of Lewis acids facilitates Pd-catalyzed directed alkenylation and acylation of acetanilide and urea derivatives.[55-57] In these studies, they demonstrated that various Lewis acid additives, including electron-deficient triaryl borane, trihalo-boranes, and inorganic metal salts with weakly coordinating anions, accelerate Pd-catalyzed C–H activation.[55-57] Similarly, in a study from the Goldberg and Goldman groups, Ir-catalyzed reactions were accelerated by the addition of sodium tetrakis[3,5-bis(trifluoromethyl)phenyl]borate as well as other Lewis acids.[58] DFT calculations showed that the Lewis acidic Na^+ cation likely promotes a κ^2 to κ^1 change for coordinated acetate leading to a vacant coordination site that accelerates the overall reaction.[58] Inspired by these studies and motivated by our recent reports of rhodium-catalyzed arene C–H activation and alkenylation chemistry,[59-69] we sought to study the influence of additives on rhodium-catalyzed arene C–H activation. To do so, we decided to test additives for the H/D exchange of toluene-d_8 in weak protio-acidic environment using 2,6-bis-(disubstituted-phosphinomethyl)pyridine (^{R}PNP) ligated Rh carboxylate complexes.

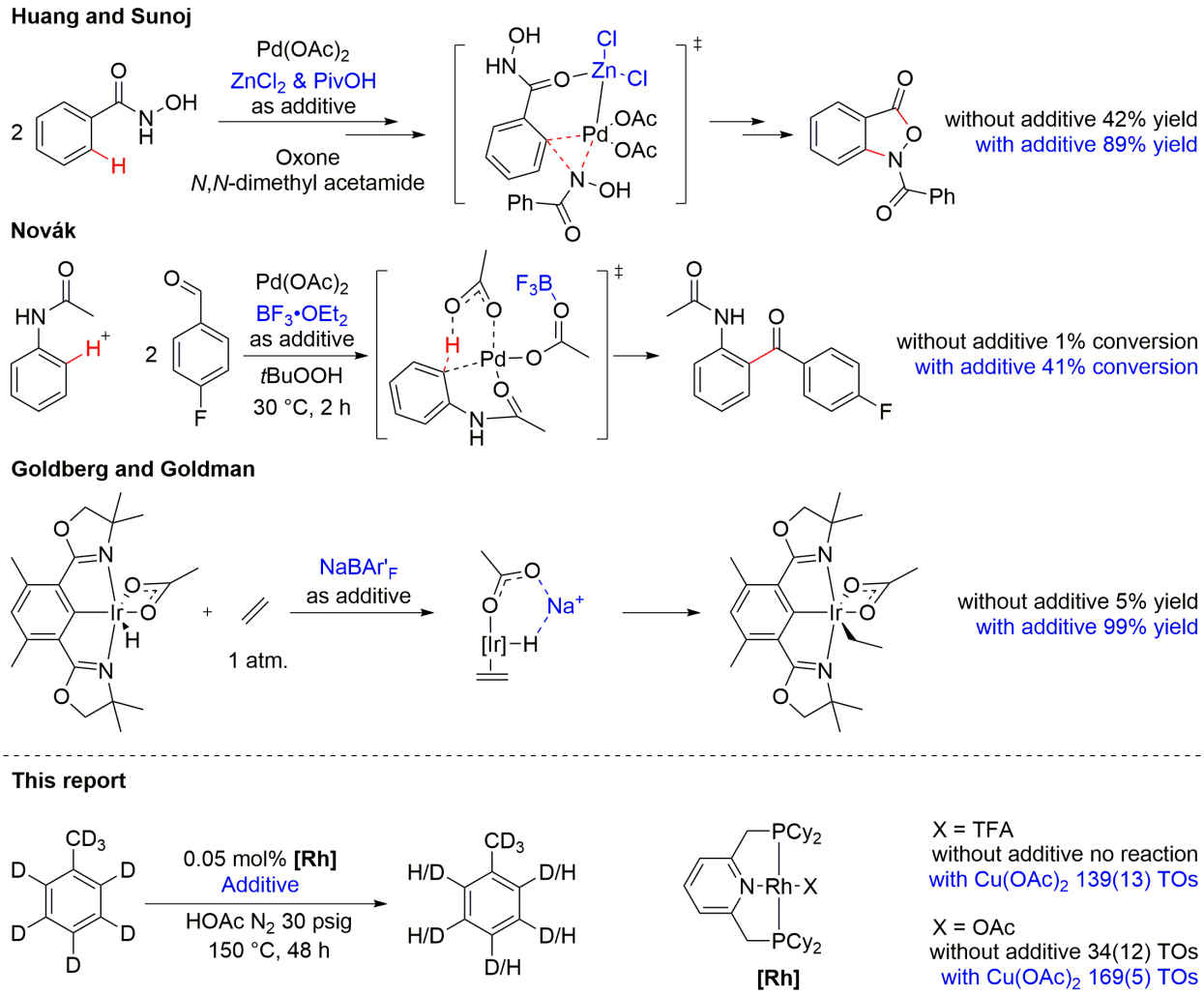

Scheme 1. Examples of previously reported Lewis acid facilitated C–H activation and this work.

Hydrogen–deuterium exchange (H/D exchange) of C–H bonds in the presence of a deuterium source (e.g., often a deuterated acid) is a tool for studying the transition metal-catalyzed C–H activation processes.[70-78] However, the result of H/D exchange catalysis with arenes in acidic media should be interpreted with caution, since the acidity of a transition metal complex can lead to the exchange via a protic aromatic substitution mechanism ($^{Ar}S_E$, Lewis acid catalyzed, electrophilic aromatic substitution with no M–C bond formation), and in such cases the rate of H/D exchange is not a measure of transition metal-mediated C−H activation reactivity (with M–C bond formation).[79] Toluene is a useful probe for transition metal mediated C–H activation versus

acid catalysis since the regioselectivity can differentiate the two processes (Scheme 2). In our previous work, we studied C–H activation using H/D exchange reactions of arenes in a strongly acidic media, which allowed for *in situ* monitoring of the selectivity and reactivity of the arene C–H activation process.[79-80] When using trifluoroacetic acid (HTFA) with a series of diimine (diazabutadienes) ligated Rh^{I} complexes, the mechanism of the arene H/D exchange reactions most likely involves protic aromatic substitution (Scheme 2a). However, when using acetic acid (HOAc), pathways such as organometallic C−H activation (Scheme 2b) might become more favorable due to the weaker acidity of HOAc.

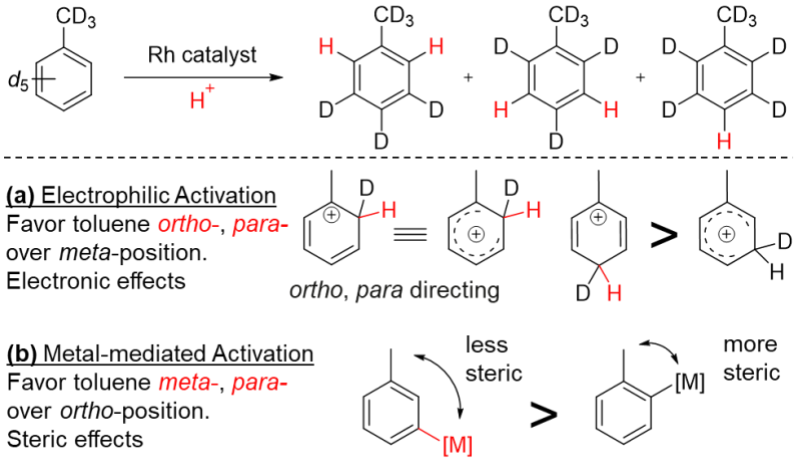

Scheme 2. Using toluene as a probe to study the metal-catalyzed C–H activation processes.

For this study, (^{R}PNP)Rh complexes were chosen due to the thermostability offered by the tridentate PNP ligand and the tunable steric and electronic properties offered by the phosphine substituents.[33-34,81-83] In addition, the presence of the phosphine moiety in the ^{R}PNP could provide information for determination of the Rh oxidation state of the reaction intermediates via ^{31}P NMR spectroscopy. Also, an example of H/D exchange between arenes and water using ($^{t\text{Bu}}$PNP)Rh(OAc) has been reported by the Goldberg group.[58]

Results and Discussion

Synthesis of Rh complexes. The ^{R}PNP ligated Rh^{I} carboxylate complexes (^{R}PNP)Rh(X) (X = TFA or OAc) (**1**-**3**) were synthesized by the reaction of free ^{R}PNP pincer pro-ligand with [Rh(η^2-C_2H_4)$_2$(μ-TFA)]$_2$ or [Rh(η^2-C_2H_4)$_2$(μ-OAc)]$_2$ in tetrahydrofuran (THF). NMR spectra of the ($^{t\text{Bu}}$PNP)Rh(X) complexes **3a**-**b** matched published data.[84] The complex [(^{R}PNP)Rh(η^2-C_2H_4)][TFA] was observed as a reaction intermediate, and the solid-state structure of [($^{t\text{Bu}}$PNP)Rh(η^2-C_2H_4)][TFA] was obtained by single crystal X-ray crystallography (see Figure S1). Also, the structures of (^{R}PNP)Rh(TFA) (R = isopropyl and *tert*-butyl) were confirmed by single crystal X-ray crystallography (see Figures S2 and S3). The Rh hydride complexes (^{R}PNP)Rh(H)(TFA)$_2$ (**4**-**6a**) were synthesized by oxidizing the corresponding (^{R}PNP)Rh(TFA) complexes with HTFA (Scheme 3). The solid-state structures of ($^{i\text{Pr}}$PNP)Rh(H)(TFA)$_2$ (**5a**) and ($^{t\text{Bu}}$PNP)Rh(H)(TFA)$_2$ (**6a**) were confirmed by single crystal X-ray crystallography, in which the hydride ligands were located in the electron density map (Figure 1). Both of the structures for **5a** and **6a** reveal that the hydride ligand is *cis* to the pyridyl N, giving a 88(2)° N1–Rh1–H1 bond angle for **5a** and 93(1)° for **6a**. The Rh1–O1 bond *trans* to the hydride has a longer bond length (2.222(2) Å for **5a**, 2.262(2) Å for **6a**) compared to the Rh1–O3 bond (2.054(2) Å for **5a**, 2.054(2) Å for **6a**) due to the *trans* influence of the hydride ligand. The Rh1–H1 bond length is 1.41(3) Å in **5a**, 1.43(3) Å in **6a**, which is reasonable compared to other published examples of (^{R}PNP)Rh^{III}–H complexes (1.46 – 1.49 Å).[85-87]

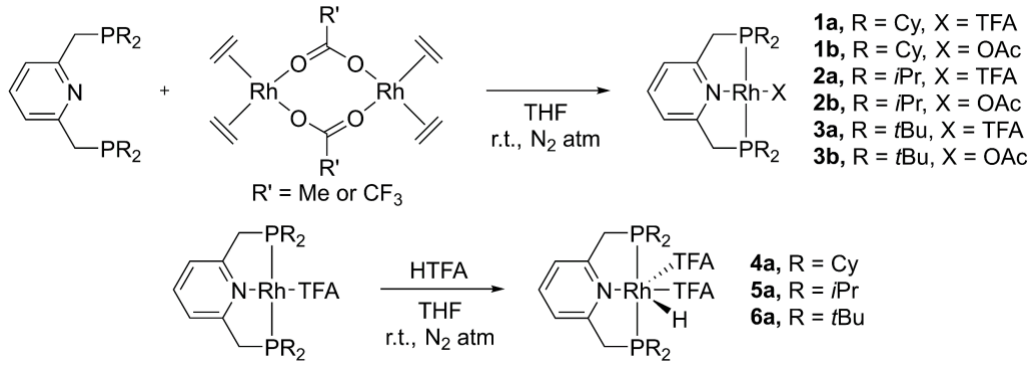

Scheme 3. Synthesis of (^{R}PNP)Rh carboxylate complexes.

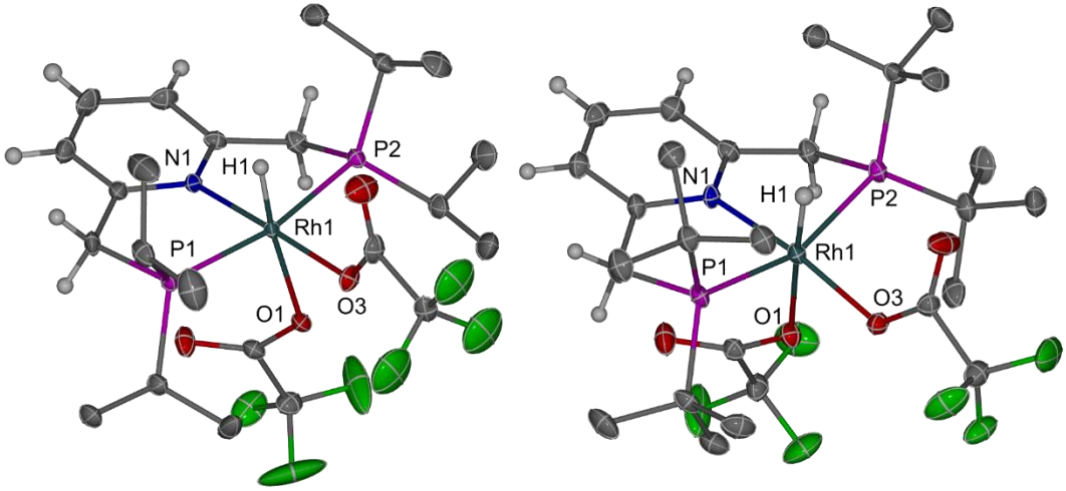

Figure 1. ORTEPs of ($^{i\text{Pr}}$PNP)Rh(H)(TFA)$_2$ (**5a**) and ($^{t\text{Bu}}$PNP)Rh(H)(TFA)$_2$ (**6a**). Ellipsoids are drawn at 50% probability level. Some of the hydrogen atoms and solvent molecule have been removed for clarity. The hydride ligands were located based on the electron density map. Selected bond lengths for **5a** (Å): Rh1–H1 1.41(3), Rh1–N1 2.052(2), Rh1–P1 2.297(1), Rh1–P2 2.314(1), Rh1–O1 2.222(2), Rh1–O3 2.054(2). Selected bond angles for **5a** (°): N1–Rh1–H1 88(2), N1–Rh1–P1 84.7(1), H1–Rh1–P1 86(1), N1–Rh1–P2 84.1(1), H1–Rh1–P2 89(1), P1–Rh1–P2 168.0(0). Selected bond lengths for **6a** (Å): Rh1–H1 1.43(3), Rh1–N1 2.038(2), Rh1–P1 2.325(1), Rh1–P2 2.352(1), Rh1–O1 2.262(2), Rh1–O3 2.054(2). Selected bond angles for **6a** (°): N1–Rh1–H1 93(1), N1–Rh1–P1 84.6(1), H1–Rh1–P1 82(1), N1–Rh1–P2 84.2(1), H1–Rh1–P2 83(1), P1–Rh1–P2 160.6(0).

Additive screening for toluene-d_8 H/D exchange. Through screening initial reaction conditions, it was determined that a combination of toluene-d_8 and HOAc in a 10:1 volume ratio provided peak separation between the *ortho*-, *meta*-, and *para*-positions (^{1}H NMR spectra) of the residual protons of toluene-d_8 with useful signal-to-noise ratio. In addition, the use of excess arene with a small amount of acid provides similar conditions to our previously published arene

alkenylation chemistry.[59-61,88] Under these conditions, the effect of different additives were tested for H/D exchange between toluene-d_8 and HOAc with or without (^{Cy}PNP)Rh(TFA) (**1a**) as the pre-catalyst. The turnovers (TOs) and regioselectivity of H/D exchange were determined by monitoring the integration change of the residual proton peaks on toluene-d_8 in ^{1}H NMR spectra. The obtained *meta*-to-*ortho* ratio (*m*/*o*) of the residual protons on toluene-d_8 and TOs of the major H/D exchange products (*meta*- or *ortho*-H/D exchange products) at 2 h and 8 h are listed in Table 1. In our previous work, HTFA was used as the proton source for H/D exchange of toluene-d_8, which gave *ortho*- and *para*-H/D exchange via a proposed electrophilic aromatic substitution mechanism without forming a M–C bond (Scheme 2a).[79-80] In contrast, a background reaction using only HOAc and toluene-d_8 gave no H/D exchange after heating at 150 °C for 8 h (Table 1, entry 1). Likewise, using **1a** in the absence of additive did not result in the activation of toluene C–H bonds to give the H/D exchange products (Table 1, entry 2).

When using Lewis acids such as $ZnCl_2$ and $BF_3{\cdot}OEt_2$, in the absence of the Rh pre-catalyst, *ortho*-selective H/D exchange was observed (Table 1, entries 3 and 4). Therefore, it can be assumed that Lewis acids such as BF_3 and $ZnCl_2$ can catalyze electrophilic aromatic protonation of toluene-d_8 with HOAc, which is consistent with previous results.[79-80] Similarly, using Lewis acids such as $BF_3{\cdot}OEt_2$ in the presence of Rh complex **1a**, the H/D exchange remained selective for the *ortho*-position of toluene, and no significant difference in the exchange rate was observed between the reaction with or without **1a** (Table 1, entry 5). In contrast, a weaker Lewis acid compared to $BF_3{\cdot}OEt_2$, $B(OMe)_3$, did not catalyze H/D exchange between toluene-d_8 and HOAc in the absence of **1a** (Table 1, entry 6). But, using a combination of $B(OMe)_3$ with **1a** provided *meta*-selective H/D exchange with 5(1) TOs of the *meta*-protonation product after heating at 150 °C for 2 hours, which presumably is a result of a Rh-mediated reaction with formation of Rh-tolyl intermediates

that favors the *meta*- over the *ortho*-position of toluene due to the steric effect of the methyl group.[76,89-92] However, extension of the reaction time to 8 hours resulted in only 6(1) TOs with the *m*/*o* of the residual protons on toluene-d_8 remaining the same as the 2 h timepoint within standard deviation (Table 1, entry 7). Thus, additional H/D exchange after 2 hours does not occur or is minimal, which is likely due to the decomposition of $B(OMe)_3$ as monitored by ^1H NMR spectroscopy (see Figure S5). Also, the formation of black precipitate on the side of the NMR tube was observed, which is likely due to the decomposition of **1a** to inactive Rh(s).

Lewis acids that are also commonly used oxidants, such as $Cu(OAc)_2$ and AgOAc, were tested for the H/D exchange of toluene-d_8 with HOAc. No reaction was observed for control reactions using $Cu(OAc)_2$ or AgOAc in the absence of Rh catalyst (Table 1, entries 8 and 9). Using $Cu(OAc)_2$ as an additive with the Rh complex **1a** resulted in *meta*-selective H/D exchange of toluene-d_8 with 16(1) TOs at 2 h and 26(1) TOs at 8 h (Table 1, entry 10). The control reaction using free ^{Cy}PNP ligand in the presence of $Cu(OAc)_2$ showed no H/D exchange of toluene-d_8 (Table 1, entry 11). Therefore, the observed H/D exchange using **1a** and $Cu(OAc)_2$ is not likely catalyzed by free ^{Cy}PNP ligand or ^{Cy}PNP ligated Cu complex. The combination of AgOAc with **1a** was also examined, and, similar to $Cu(OAc)_2$, *meta*-selective H/D exchange was found with 6(0) TOs at 2 h and 12(1) TOs at 8 h (Table 1, entry 12). Based on these results, it can be hypothesized that Cu^{II} and Ag^{I} have a positive effect on rhodium-catalyzed C–H activation of toluene that likely occurs via an organometallic pathway with Rh-tolyl intermediates. It is likely that the Cu^{II} and Ag^{I} salts prevent the formation of inactive Rh(s) (see below for more discussion).[59]

A common reducing agent that also serves as a Lewis acid, $SnCl_2$, was also tested, which resulted in *ortho*-selective H/D exchange of toluene-d_8 (Table 1, entry 13). It is possible that $SnCl_2$ serves as a Lewis acid catalyst or that the Sn^{II} is oxidized under acidic conditions to generate a

high valent Sn^{IV} Lewis acid catalyst to facilitate the electrophilic aromatic protonation of toluene-d_8. Similarly, using $SnCl_2$ as an additive in the presence of pre-catalyst **1a** resulted in *ortho*-selective H/D exchange (Table 1, entry 14). Thus, in the presence of $SnCl_2$ no evidence of Rh-mediated H/D exchange is found. A different Cu^{II} salt, $CuCl_2$, was also examined with and without **1a** aiming to confirm the necessity of using the oxidizing cation in the (^{R}PNP)Rh-mediated H/D exchange; however, no H/D exchange was observed, possibly attributable to the low solubility of $CuCl_2$ (Table 1, entries 15 and 16). Alternatively, using the soluble $AgBF_4$ in the presence of **1a** provided *meta*-selective H/D exchange with 6(1) TOs at 2 h and 23(2) TOs at 8 h as expected (Table 1, entry 17). When using a non-oxidizing magnesium salt, $MgSO_4$, no H/D exchange was observed with or without **1a** (Table 1, entries 18 and 19). Also, using CuOAc gave no H/D exchange of toluene-d_8 (Table 1, entry 20), and the combination of CuOAc with **1a** resulted in *meta*-selective H/D exchange with lower TOs (11(1) at 8 h) (Table 1, entry 21) compared to $Cu(OAc)_2$. It remains unclear whether the observed H/D exchange of toluene-d_8 is facilitated by the CuOAc or Cu^{II} that is potentially formed from the disproportionation of CuOAc under the reaction conditions.[93-95]

Table 1. Initial additive screening for H/D exchange between toluene-d_8 and HOAc using (^{Cy}PNP)Rh(TFA) (**1a**) as the pre-catalyst.

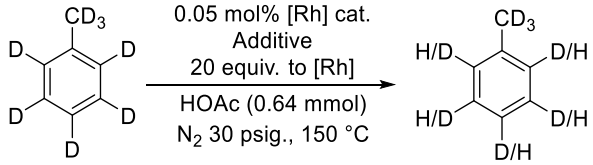

3.42 mmol

Entry	[Rh] pre-catalyst	Additive	Selectivity	*m*/*o* (2 h)	TOs (2 h)	*m*/*o* (8 h)	TOs (8 h)
1	None	None	*NA*	0.97(0)	*NA*	0.97(0)	*NA*
2	**1a**	None	*NA*	1.01(2)	*NA*	1.00(0)	*NA*
3[a]	None	$ZnCl_2$	*ortho*	0.31(3)	99(3)	0.21(1)	203(16)
4[a]	None	$BF_3{\cdot}OEt_2$	*ortho*	0.75	3	0.67	6
5	**1a**	$BF_3{\cdot}OEt_2$	*ortho*	0.77(2)	5(2)	0.74(1)	9(2)

6	None	$B(OMe)_3$	*NA*	0.97	*NA*	1.00	*NA*
7	**1a**	$B(OMe)_3$	*meta*	1.24(3)	5(1)	1.21(2)	6(1)
8	None	$Cu(OAc)_2$	*NA*	1.01(2)	*NA*	1.00(2)	*NA*
9	None	AgOAc	*NA*	0.96(0)	*NA*	0.96(0)	*NA*
10	**1a**	$Cu(OAc)_2$	*meta*	1.72(7)	16(1)	2.24(9)	26(1)
11	^{Cy}PNP	$Cu(OAc)_2$	*NA*	0.96(7)	*NA*	1.01(3)	*NA*
12	**1a**	AgOAc	*meta*	1.21(2)	6(0)	1.75(4)	12(1)
13[a]	None	$SnCl_2$	*ortho*	0.94(5)	2(1)	0.83(5)	3(1)
14	**1a**	$SnCl_2$	*ortho*	0.90(4)	2(0)	0.75(8)	9(4)
15	None	$CuCl_2$	*NA*	1.02(8)	*NA*	1.06(8)	*NA*
16	**1a**	$CuCl_2$	*NA*	1.00(6)	*NA*	1.04(8)	*NA*
17	**1a**	$AgBF_4$	*meta*	1.40(1)	6(1)	2.27(11)	23(2)
18[b]	None	$MgSO_4$	*NA*	1.00(0)	*NA*	0.98(1)	*NA*
19[b]	**1a**	$MgSO_4$	*NA*	1.13(1)	1(1)	1.09(4)	2(2)
20[b]	None	CuOAc	*NA*	1.00(1)	*NA*	1.01(1)	*NA*
21[c]	**1a**	CuOAc	*meta*	1.19(3)	10(1)	1.26(3)	11(1)
22[b]	None	$Pb(OAc)_2$	*NA*	0.98(0)	*NA*	0.98(0)	*NA*
23[c]	**1a**	$Pb(OAc)_2$	*NA*	1.03(0)	*NA*	1.04(1)	*NA*
24	**1a**	NaOAc	*meta*	2.0(4)	9(4)	2.1(6)	12(2)

Reaction conditions: toluene-d_8 (0.36 mL, 3.42 mmol), HOAc (0.64 mmol), **1a** (1.7 μmol), additive (34 μmol), 150 °C, 30 psig N_2; *NA* = not applicable (i.e., no H/D exchange observed). Standard deviations are calculated from at least three independent experiments. [a] TOs of the major product were calculated based on Rh concentration used for other experiments for direction comparison; [b] using *m*/*o* ratio at 24 h and 48 h; [c] using *m*/*o* ratio at 4 h and 8 h.

In order to study the effect of the acetate anion with a non-oxidizing salt, $Pb(OAc)_2$ was examined with and without **1a**. In both cases H/D exchange of toluene-d_8 was not observed (Table 1, entries 22 and 23). But, the use of NaOAc with **1a** resulted in *meta*-selective H/D exchange with 9(4) TOs at 2 h and 12(2) TOs at 8 h (Table 1, entry 24). Similar to the H/D exchange reaction using $B(OMe)_3$ as the additive, the TOs of *meta*-protonation product and the *m/o* ratio of the residual protons on toluene-d_8 remained the same after heating for 2 hours (within standard deviation). The formation of black precipitate was also observed. Consequently, it can be hypothesized that Na^+ cation may serve as a Lewis acid similar to $B(OMe)_3$ that facilitates the Rh-mediated H/D exchange of toluene-d_8, but the reaction stops within 2 hours due to the possible decomposition of **1a** to inactive Rh(s) (see below).

Based on the screening results, all of the additives that provided *meta*-selective H/D exchange of toluene-d_8 with HOAc are listed in Table 2 and Figure 2 along with the TOs of *ortho*-, *meta*-, and *para*-H/D exchange. For each reaction listed in Table 2, no significant H/D exchange was found at the toluene benzylic position. Since the toluene benzylic C–H bonds (~88 kcal/mol) are weaker than the arene C–H bonds (~110 kcal/mol), pathways involving the generation of free radicals that are responsible for C–D activation are unlikely. For the trials using paramagnetic Cu^{II} salt, no activity for H/D exchange at the benzylic position was confirmed by ^{1}H and ^{13}C NMR spectroscopy (see Supporting Information, Section 3.5) after the consumption of all the Cu^{II} salt (based on the change in solution color from green to yellow, and the disappearance of line broadening of OAc-CH_3 peak caused by the Cu^{II} in ^{1}H NMR spectra). When using non-oxidizing additives, such as $B(OMe)_3$ or NaOAc with **1a**, the H/D exchange of toluene-d_8 with HOAc after 8 hours resulted in more proton incorporation on the *meta*- over the *para*-position with an approximate 2:1 ratio (Table 2, entries 1 and 5), which could be explained by the statistical preference of the *meta*- over the *para*-position of toluene-d_8. After taking account of the statistical ratio, there is no significant preference between reaction at the *meta*- and *para*-positions, and thus similar activation barriers for *meta* and *para* C–H activation for the Rh-mediated H/D exchange are likely. Similar *meta* to *para* selectivity has been observed in our previous work on rhodium-catalyzed alkenylation of toluene with 1-pentene,[60] and other published organometallic C−H activation processes involving toluene.[89,92,96]

In contrast to selectivity with $B(OMe)_3$ and NaOAc, using additives such as Cu^{II} and Ag^{I} in the presence of pre-catalyst **1a** results in nearly equal TOs of H/D exchange at the *meta*- and *para*-positions of toluene-d_8 (Table 2, entries 2-4). Thus, in the presence of Cu^{II} or Ag^{I} additive, after adjustment for the statistical ratio, the H/D exchange of toluene demonstrates a preference for the

para- over the *meta*- position. Similar *meta*/*para* selectivity has been observed in our previous work on rhodium-catalyzed alkenylation of toluene with propene in the presence of $Cu(OAc)_2$.[62] We presume that the presence of Cu^{II} could lead to a more sterically controlled reaction pathway compared to the H/D exchange using non-oxidizing additives such as NaOAc, and thus the less steric hindered *para*-position on toluene is favored. However, we are unable to provide a detailed explanation of these selectivity patterns. Reacting CuOAc with **1a** gave *meta*-*para*-selective H/D exchange with an approximate 1.4:1 ratio of *meta* to *para* (Table 2, entry 5), and the (*m*+*p*)/*o* ratio (~3:1) is much lower than using $Cu(OAc)_2$ {(*m*+*p*)/*o* = ~10:1}.

Table 2. Turnovers of H/D exchange between toluene-d_8 and HOAc using different additives with (^{Cy}PNP)Rh(TFA) (**1a**) as the pre-catalyst.

Entry	[Rh] pre-catalyst	Additive	TOs at 2 h (*o*:*m*:*p*)	TOs at 8 h (*o*:*m*:*p*)
1	**1a**	$B(OMe)_3$	3(1):5(1):2(0)	4(1):6(1):3(1)
2	**1a**	$Cu(OAc)_2$	4(2):16(1):16(2)	5(2):26(1):25(1)
3	**1a**	AgOAc	3(0):6(0):4(0)	3(1):12(1):10(0)
4	**1a**	$AgBF_4$	1(1):6(1):7(0)	4(1):23(2):25(2)
5	**1a**	NaOAc	1(1):9(4):3(1)	2(1):12(2):5(1)
6[a]	**1a**	CuOAc	6(1):10(1):7(1)	6(0):11(1):8(1)

Reaction conditions: toluene-d_8 (0.36 mL, 3.42 mmol), HOAc (0.64 mmol), **1a** (1.7 μmol), additive (34 μmol), 150 °C, 30 psig N_2; Standard deviations are calculated from at least three independent experiments.

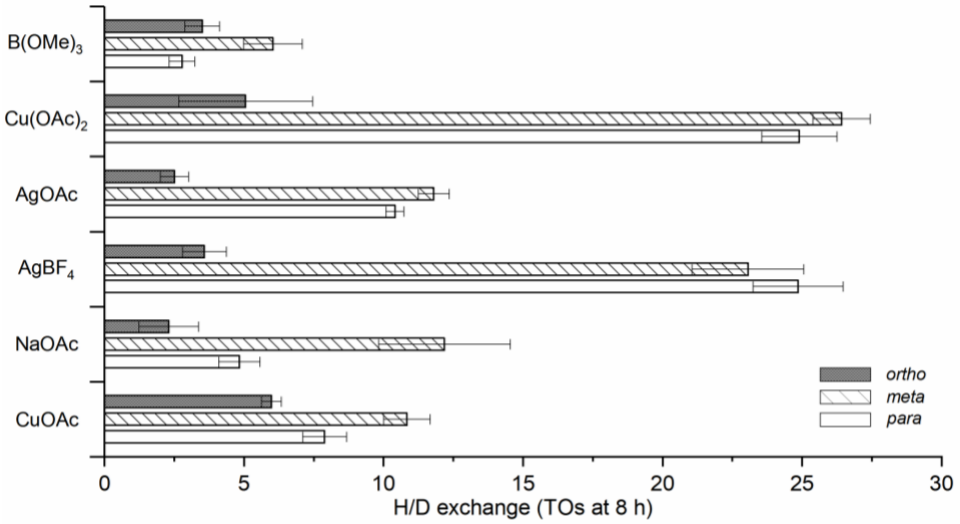

Figure 2. Comparison of H/D exchange selectivity between toluene-d_8 and HOAc using different additives with **1a**. Standard deviations are calculated from at least three independent experiments.

Based on the additive screening results, a few conclusions can be drawn (Scheme 4): (1) Lewis acids (such as BF_3) with or without pre-catalyst **1a** give *ortho-para*-selective H/D exchange that likely occurs via electrophilic aromatic protonation; (2) the combination of Lewis acids such as $B(OMe)_3$ or NaOAc with pre-catalyst **1a** show a short-lived *meta-para*-selective H/D exchange of toluene-d_8 that likely occurs by a Rh-mediated pathway with an approximate 2:1 *meta/para* ratio, but rapid catalyst deactivation occurs {likely through the formation of Rh(s)}; (3) using additives, such as $Cu(OAc)_2$ or AgOAc with **1a** provided *meta-para*-selective H/D exchange with the highest TOs of any catalyst combination with an approximate 1:1 *meta*/*para* ratio. Based on previous observations,[59] in combination with these new results, we speculate that the Cu^{II} or Ag^{I} additives likely prevent decomposition of molecular Rh to form inactive Rh(s) species.

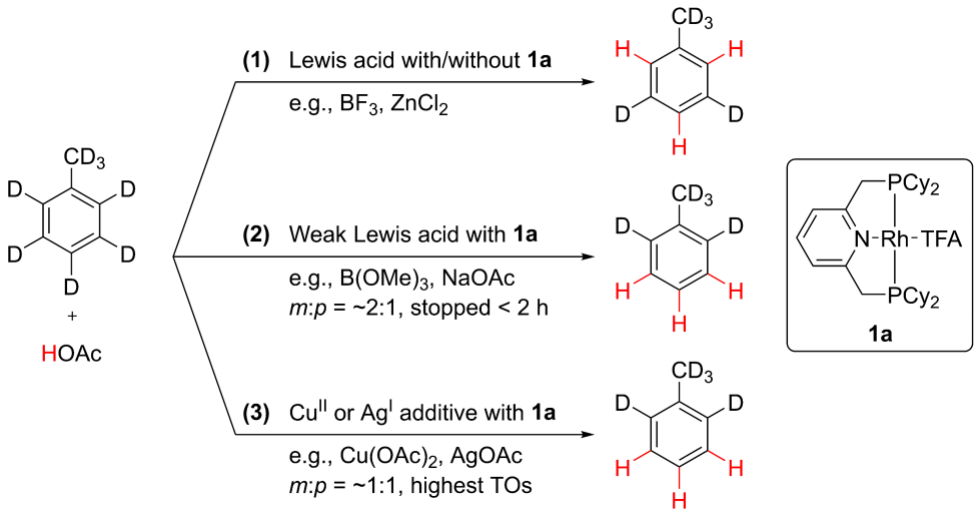

Scheme 4. Effects of various Lewis acid additives in H/D exchange of toluene-d_8 with HOAc using **1a**.

Screening different ^{R}PNP ligated Rh complexes. A series of ^{R}PNP ligated Rh(TFA) complexes (**1-3a**) were synthesized and tested for H/D exchange using $Cu(OAc)_2$ as the additive with extended reaction time compared to the additive screening. The TOs of H/D exchange at the *ortho*-, *meta*-, and *para*-position of toluene-d_8 were monitored at 8 h, 24 h and 48 h (Table 3, Figure 3). The acetate complexes (^{R}PNP)Rh(OAc) (**1-3b**) were also synthesized and tested for catalytic H/D exchange (Table 4, Figure 4). Among the three tested Rh(TFA) complexes (**1-3a**), complex **1a** as precursor gave rise to the most efficient catalysis, with 68(6) TOs of H/D exchange at the toluene-d_8 *meta*-position and 62(5) TOs at the *para*-position after heating for 48 hours (Table 3, entry 1). The pre-catalyst **3a** showed moderate activity (40(2) TOs at the *meta*-position and 42(2) TOs at the *para*-position at 48 h, Table 3, entry 3), while complex **2a** gave the lowest TOs (20(2) TOs at the *meta*-position and 17(2) TOs at the *para*-position at 48 h, Table 3, entry 2). Similar to **1a**, the control experiment using **3a** without $Cu(OAc)_2$ did not lead to statistically significant difference in the integration of the residual proton peaks of toluene-d_8. Different from **1a** and **3a**, using **2a** without additive did catalyze H/D exchange of toluene-d_8 with HOAc. However, the reaction is short-lived, and no further reaction was observed after 8 hours (only 7(1) TOs on *meta*-

position and 3(1) TOs on *para*-position at 48 h, Table 3, Entry 4), along with the formation of a black precipitate on the side of NMR tube, likely due to the decomposition of catalyst **2a** to inactive Rh(s) species. For the reaction of toluene-d_8 with HOAc using **2a** without additives, the black precipitate was isolated and studied with transmission electron microscopy (TEM), which showed a nanoparticle aggregation morphology under electron illumination (see Figure S26). In addition, the H/D exchange without the Cu^{II} salt showed an enhanced preference for the *meta*- (compared with *para*-selectivity) with *meta*/*para* > 2:1, whereas in the presence of $Cu(OAc)_2$ an equal amount of H/D exchange on the *meta*- and *para*-positions was observed. Thus, we anticipate that the actual catalyst in the H/D exchange could be different with and without the presence of $Cu(OAc)_2$. This is perhaps expected since Lewis acids are known to bind to ligands and alter the electron density of the metal center.[97] For the (^{R}PNP)Rh catalysts, Lewis acids could potentially bond to carboxylate ligands.

Table 3. Turnovers of H/D exchange between toluene-d_8 and HOAc using (^{Cy}PNP)Rh(TFA) (**1a**), ($^{i\text{Pr}}$PNP)Rh(TFA) (**2a**), and ($^{t\text{Bu}}$PNP)Rh(TFA) (**3a**) as the pre-catalysts.

Entry	[Rh] pre-catalyst	Additive	TOs at 8 h (*o*:*m*:*p*)	TOs at 24 h (*o*:*m*:*p*)	TOs at 48 h (*o*:*m*:*p*)
1	**1a**	$Cu(OAc)_2$	5(2):26(1):25(1)	7(3):43(3):41(2)	10(3):68(6):62(5)
2	**2a**	$Cu(OAc)_2$	5(2):12(3):9(2)	5(1):15(2):13(1)	6(1):20(2):17(2)
3	**3a**	$Cu(OAc)_2$	3(1):19(2):20(2)	3(0):27(2):29(3)	4(0):40(2):42(2)
4	**2a**	None	2(1):8(2):3(1)	2(1):9(2):3(1)	1(1):7(1):3(1)

Reaction conditions: toluene-d_8 (0.36 mL, 3.42 mmol), HOAc (0.64 mmol), Rh pre-catalyst (1.7 μmol), $Cu(OAc)_2$ (34 μmol), 150 °C, 30 psig N_2; Standard deviations are calculated from at least three independent experiments.

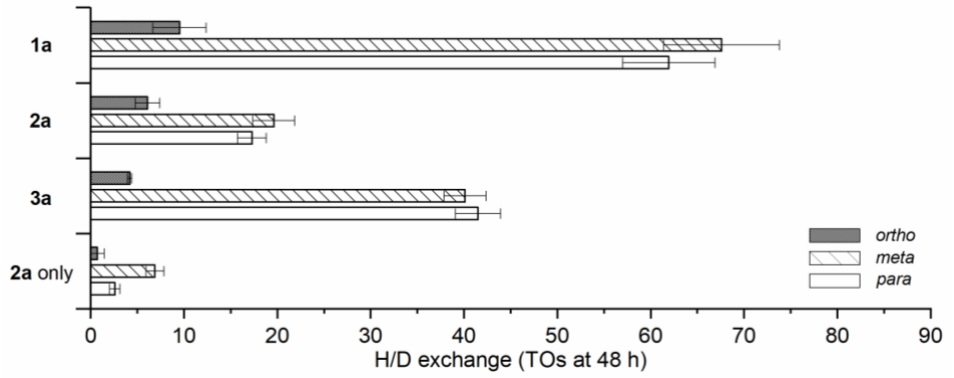

Figure 3. Comparison of H/D exchange between toluene-d_8 and HOAc using (^{Cy}PNP)Rh(TFA) (**1a**), (^{iPr}PNP)Rh(TFA) (**2a**) and (^{tBu}PNP)Rh(TFA) (**3a**) as the pre-catalysts. Standard deviations are calculated from at least three independent experiments.

The effect of ligand choice was observed, where the apparent turnover frequencies (TOFs) of substituted (^{R}PNP)Rh(TFA) catalyzed H/D exchange followed a trend of (^{Cy}PNP)Rh(TFA) (**1a**) > (^{tBu}PNP)Rh(TFA) (**3a**) > (^{iPr}PNP)Rh(TFA) (**2a**) (Table 5). This observed ligand effect provides evidence against the likelihood of a simple Rh species, formed by fast ligand dissociation, serving as the actual catalyst, which we have observed for Rh catalyzed arene alkenylation.[59-60] The proposal that the (^{R}PNP)Rh complexes are responsible for the catalytic H/D exchange is also consistent with (*m*+*p*)/*o* ratio as a function of ligand identity. The H/D exchange using the bulkiest ligand, complex **3a**, resulted in a higher (*m*+*p*)/*o* ratio (~21:1) compared to the other two: the observed (*m*+*p*)/*o* ratios were ~13:1 for **1a** and ~6:1 for **2a**. Complex **3a** showed an H/D exchange rate intermediate between **1a** and **2a**. This is perhaps expected since the bulkier substituents also tend to increase the Rh–P distances, and likely diminishes the electronic effect along with the steric impact. Indeed, based on the X-ray crystal structures, the Rh–P distances in the (^{tBu}PNP)Rh complexes are longer than that in the (^{iPr}PNP)Rh complexes (Rh–P distances (Å): 2.2738(9) and 2.2842(9) in **3a** vs. 2.2679(4) and 2.2742(4) in **2a**; 2.3250(6) and 2.3518(6) in **6a** vs. 2.2966(8) and 2.3140(8) in **5a**). Thus, discerning kinetic trends based on the ligand steric influence is not straightforward.

Using the acetate complexes (^{R}PNP)Rh(OAc) (**1-3b**) as the pre-catalysts, the TOs of H/D exchange at the *ortho*-, *meta*-, and *para*-position of toluene-d_8 were monitored at 8 h, 24 h and 48 h (Table 4, Figure 4). Under the conditions in the presence of $Cu(OAc)_2$ as the additive, the observed TOFs of H/D exchange using (^{R}PNP)Rh(OAc) follows the same trend (**1b** > **3b** > **2b**) (Table 5) as the (^{R}PNP)Rh(TFA) pre-catalysts. The H/D exchange using isopropyl substituted (^{R}PNP)Rh complex **2b** showed the lowest TOs (15(4) on *meta*-position and 9(3) TOs on *para*-position at 48 h, Table 4, entry 2). A control experiment using (^{R}PNP)Rh(OAc) pre-catalysts **1-3b** without Cu^{II} salt showed activity for *meta*-selective H/D exchange of toluene-d_8 with an approximate 2:1 *meta*/*para* ratio (Table 4, entries 4-6). These results are different from the use of (^{R}PNP)Rh(TFA) as the pre-catalyst, which showed no activity (**1a** and **3a**) or very low turnovers (**2a**) for H/D exchange without additive. The catalyst activity of (^{R}PNP)Rh(OAc) followed a trend of **2b** > **1b** > **3b**, which differs from that in the presence of Cu^{II} (**1b** > **3b** > **2b**). The observed H/D exchange reactions when using (^{R}PNP)Rh(OAc) without Cu^{II} additive, stopped within 8 hours along with the formation of black precipitate. In contrast, black precipitate was not observed under the condition in the presence of the Cu^{II} additive. The presence of $Cu(OAc)_2$ substantially impacts the activity of **1b** and **3b** (Table 4, entries 1 vs 4, 3 vs 6), while it inhibits the H/D exchange using **2b** (Table 4, entries 2 vs 5). Therefore, the reactions with and without $Cu(OAc)_2$ likely undergo different pathways, and the isopropyl substituted pre-catalysts seem to be divergent from the others.

Table 4. Turnovers of H/D exchange between toluene-d_8 and HOAc using (^{Cy}PNP)Rh(OAc) (**1b**), (^{iPr}PNP)Rh(OAc) (**2b**), (^{tBu}PNP)Rh(OAc) (**3b**) and $[Rh(\eta^2\text{-}C_2H_4)_2(\mu\text{-}OAc)]_2$ (**Rh dimer**) as the pre-catalysts.

Entry	[Rh] pre-catalyst	Additive	TOs at 8 h (*o*:*m*:*p*)	TOs at 24 h (*o*:*m*:*p*)	TOs at 48 h (*o*:*m*:*p*)
1	**1b**	$Cu(OAc)_2$	5(2):27(1):25(8)	9(1):54(2):47(1)	12(1):83(3):74(2)
2	**2b**	$Cu(OAc)_2$	1(3):9(5):3(2)	1(2):11(5):6(2)	3(2):15(4):9(3)
3	**3b**	$Cu(OAc)_2$	0(0):15(1):16(1)	3(1):30(1):31(0)	3(1):41(1):41(1)
4	**1b**	None	3(1):28(8):11(3)	2(1):25(9):9(3)	1(1):24(9):9(3)

5	**2b**	None	4(1):63(7):29(4)	3(1):55(9):26(5)	4(1):57(10):27(6)
6	**3b**	None	0(2):2(1):0(1)	0(2):2(2):1(1)	0(2):5(4):2(2)
7	**Rh dimer**	$Cu(OAc)_2$	1(0):2(0):2(0)	1(1):4(1):4(1)	1(1):5(1):5(0)

Reaction conditions: toluene-d_8 (0.36 mL, 3.42 mmol), HOAc (0.64 mmol), Rh pre-catalyst (1.7 μmol, based on Rh), $Cu(OAc)_2$ (34 μmol), 150 °C, 30 psig N_2; Standard deviations are calculated from at least three independent experiments.

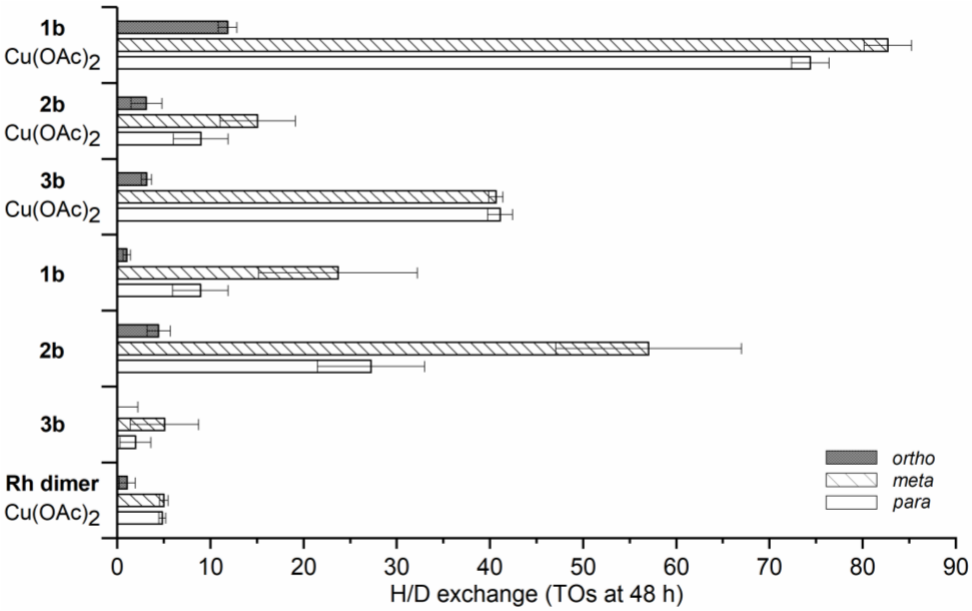

Figure 4. Comparison of H/D exchange between toluene-d_8 and HOAc using (^{Cy}PNP)Rh(OAc) (**1b**), (^{iPr}PNP)Rh(OAc) (**2b**), (^{tBu}PNP)Rh(OAc) (**3b**), and $[Rh(\eta^2\text{-}C_2H_4)_2(\mu\text{-}OAc)]_2$ (**Rh dimer**) as the pre-catalysts. Standard deviations are calculated from at least three independent experiments.

To understand the effect of carboxylate ligands, the TOs of H/D exchange showing total sp^2 data (i.e., *ortho* + *meta* + *para*) and data at the *meta* position of toluene-d_8 using (^{R}PNP)Rh pre-catalysts in the presence of $Cu(OAc)_2$ as the additive were plotted (Figure 5a-c). For all of the (^{R}PNP)Rh pre-catalysts, the resulting H/D exchange reactions were relatively fast within the initial 4–8 hours after which the rate of H/D exchange slowed, and after 12 hours a linear relation between TOs and time was observed (Figure 6). Under the reaction conditions, a maximum of 374 TOs for H/D exchange is possible (if the exchange reactions proceeded to completion). Thus, it is likely that the decrease in rate after a few hours is at least partially related to the reverse D/H exchange. Comparing the H/D exchange using the (^{Cy}PNP)Rh(TFA) (**1a**) and (^{Cy}PNP)Rh(OAc) (**1b**) as the

pre-catalyst, no significant difference was found between the reaction rates in the first 12 hours (Figure 5a). Similarly, using **3a** and **3b** also provided almost identical TOs vs time plots at the beginning (Figure 5c). These observations seem to suggest that ultimately (^{R}PNP)Rh(TFA) and (^{R}PNP)Rh(OAc) are converted to the same catalyst, which likely can be formed by two possible pathways: (1) dissociation of the carboxylate ligand leading to a cationic Rh^{I} complex serving as the catalyst, similar to the mechanism of H/D exchange between arenes and water reported by the Goldberg group.[84,98] However, during the catalysis, we observed a light-yellow color of the reaction solution, which is commonly observed for PNP ligated Rh^{III} complexes.[81-82,85,87,99] This observation is consistent with Rh^{III} as the active catalyst. (2) The pre-catalysts undergo oxidative addition of HOAc to generate Rh^{III} complexes, which serve as the active catalysts for H/D exchange (Path A in Scheme 5). The ligated carboxylate ion can exchange between TFA and OAc facilitated by the $Cu(OAc)_2$ or Lewis acid such as NaOAc and $B(OMe)_3$, so no obvious difference in H/D exchange was observed when using (^{R}PNP)Rh(TFA) and (^{R}PNP)Rh(OAc) (R = Cy or *t*Bu) in the presence of additive. Without the presence of Lewis acid additive, very slow or no H/D exchange reactions were observed using (^{R}PNP)Rh(TFA) pre-catalysts **1a**, **2a** and **3a** (Table 3, Figure 3).

In the later stages of the reaction, the catalytic H/D exchange using Rh complexes with acetate as the ligand (**1b**, **3b**) provided slightly more TOs than with TFA as the ligand (**1a**, **3a**) (Figure 5a and 5c). Although carboxylate ion exchange between OAc and TFA is likely, the presence of TFA anion in the solution may still compete with OAc coordination and lead to a slightly slower overall rate of catalytic H/D exchange in the later stage of the reaction. This can be rationalized by the basicity of carboxylate ligands. The carboxylate ligand with higher pK_a values for the corresponding RCO_2H acids (HOAc pK_a = 4.8 vs. HTFA pK_a = 0.2) is likely more active for arene

C–H activation via a potential concerted metalation deprotonation (CMD) mechanism[100-101] due to the more basic carbonyl, similar to the findings from Jones and coworkers for their Ir-catalyzed octane dehydrogenation chemistry.[102]

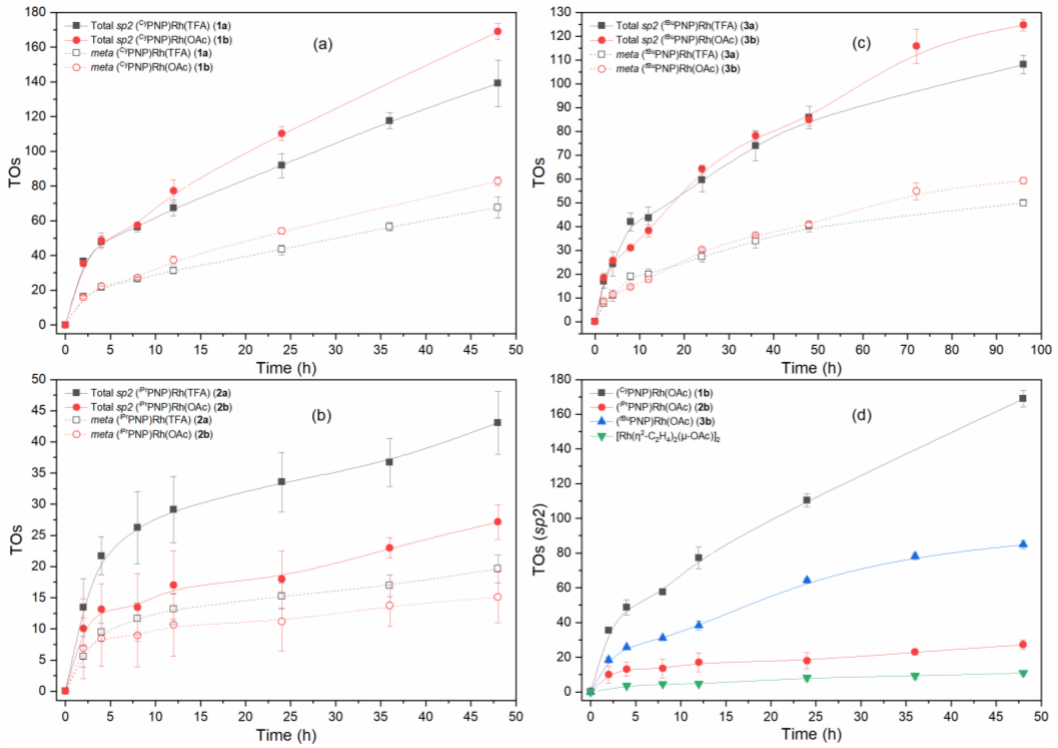

Figure 5. Comparison of TOs for H/D exchange between toluene-d_8 and HOAc showing total sp^2 data (i.e., *ortho* + *meta* + *para*) and data at the *meta* position using different Rh pre-catalysts in the presence of $Cu(OAc)_2$ as the additive. Reaction conditions: toluene-d_8 (0.36 mL, 3.42 mmol), HOAc (0.64 mmol), Rh pre-catalyst (1.7 μmol, based on Rh), $Cu(OAc)_2$ (34 μmol), 150 °C, 30 psig N_2. Standard deviations are calculated from at least three independent experiments. (a) Comparison of H/D exchange using ^{Cy}PNP ligated Rh complexes **1a** and **1b**. (b) Comparison of H/D exchange using $^{i\text{Pr}}$PNP ligated Rh complexes **2a** and **2b**. (c) Comparison of H/D exchange using $^{t\text{Bu}}$PNP ligated Rh complexes **3a** and **3b**. (d) TOs of H/D exchange on sp^2 positions using **1b**, **2b**, **3b**, and $[Rh(\eta^2\text{-}C_2H_4)_2(\mu\text{-}OAc)]_2$.

Our previous work demonstrated that activation of arene C–H bonds can be achieved using $[Rh(\eta^2\text{-}C_2H_4)_2(\mu\text{-}OAc)]_2$ as the pre-catalyst in the presence of Cu^{II} carboxylate.[59-60,62] Thus, $[Rh(\eta^2\text{-}C_2H_4)_2(\mu\text{-}OAc)]_2$ was also tested for H/D exchange (Table 4, entry 7), and the H/D exchange of toluene showed a preference for the *meta*- and *para*-positions, as expected, with a *meta*/*para* ratio of 1:1 consistent with our reported toluene alkenylation using propylene.[62]

However, after 48 hours only 5(1) TOs of H/D exchange of toluene-d_8 at the *meta*-position and 5.0(4) TOs at the *para*-position were achieved, which is significantly slower than the exchange using (^{R}PNP)Rh pre-catalysts **1a-b** and **3a-b** especially during the initial 4–8 hours (Figure 5d). In addition, differences in the exchange rates after 12 hours were observed. Using pre-catalysts **1b**, **3b** and [Rh(η^2-C_2H_4)$_2$(μ-OAc)]$_2$, the apparent TOFs of H/D exchange after 12 hours were found to be 6.6(2), 3.4(6), and 0.5(1) × 10^{-4} s^{-1} (Table 5, Figure 6). These observations support that the ^{Cy}PNP and $^{t\text{Bu}}$PNP ligands likely remain coordinated during the H/D exchange reaction, and they likely provide additional stabilization of the Rh catalyst.

Table 5. TOFs of H/D exchange between toluene-d_8 and HOAc using (^{R}PNP)Rh(X) (X = TFA or OAc, **1-3**) and [Rh(η^2-C_2H_4)$_2$(μ-OAc)]$_2$ (**Rh dimer**) as the pre-catalysts.

Entry	[Rh] pre-catalyst	Additive	Initial TOF (2 h) (s^{-1})	TOF after 12 h (s^{-1})
1	**1a**	$Cu(OAc)_2$	51(3) × 10^{-4}	5.7(1) × 10^{-4}
2	**1b**	$Cu(OAc)_2$	49(2) × 10^{-4}	6.6(2) × 10^{-4}
3	**2a**	$Cu(OAc)_2$	19(6) × 10^{-4}	0.7(1) × 10^{-4}
4	**2b**	$Cu(OAc)_2$	14(7) × 10^{-4}	0.9(0) × 10^{-4}
5	**3a**	$Cu(OAc)_2$	23(4) × 10^{-4}	3.3(1) × 10^{-4}
6	**3b**	$Cu(OAc)_2$	26(3) × 10^{-4}	3.4(6) × 10^{-4}
7	**Rh dimer**	$Cu(OAc)_2$	2(1) × 10^{-4}	0.5(1) × 10^{-4}

Reaction conditions: toluene-d_8 (0.36 mL, 3.42 mmol), HOAc (0.64 mmol), Rh pre-catalyst (1.7 μmol, based on Rh), $Cu(OAc)_2$ (34 μmol), 150 °C, 30 psig N_2; standard deviations are calculated from at least three independent experiments.

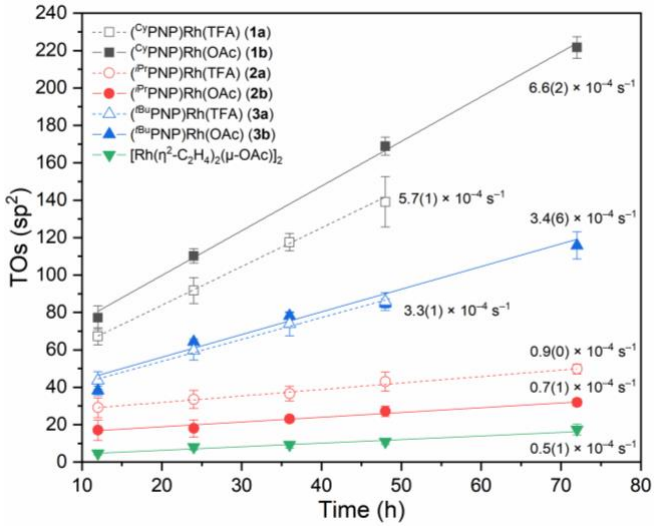

Figure 6. Plots of H/D exchange between toluene-d_8 and HOAc after 12 h using **1-3**, and [Rh(η^2-C_2H_4)$_2$(μ-OAc)]$_2$ in the presence of Cu(OAc)$_2$ as additive. Reaction condition: toluene-d_8 (0.36 mL, 3.42 mmol), HOAc (0.64 mmol), Rh pre-catalyst (1.7 μmol), Cu(OAc)$_2$ (34 μmol), 150 °C, 30 psig N_2. Standard deviations are calculated from at least three independent experiments.

Results for the H/D exchange reactions using ($^{i\text{Pr}}$PNP)Rh complexes **2a** and **2b** are different from using other ($^{\text{R}}$PNP)Rh complexes (Figure 5b). A faster rate of H/D exchange was found using the ($^{i\text{Pr}}$PNP)Rh(TFA) complex **2a** compared to the same reactions using ($^{i\text{Pr}}$PNP)Rh(OAc) (**2b**), especially within the first 4–8 hours. For H/D exchange using **2b**, the apparent TOF calculated after 12 hours was found to be 0.7(1) × 10^{-4} s^{-1}, which is statistically the same as that using [Rh(η^2-C_2H_4)$_2$(μ-OAc)]$_2$ (0.5(1) × 10^{-4} s^{-1}). Therefore, we suspect that the active ($^{i\text{Pr}}$PNP)Rh intermediate decomposes to inactive Rh(s) species within the first few hours. Perhaps continued H/D exchange after catalyst decomposition is due to small amounts of leached Rh from the Rh(s), similar to our previous studies of Rh catalyzed arene alkenylation.[59] For **2a**, a slightly greater TOF was calculated (0.9(0) × 10^{-4} s^{-1}) after 12 h. We hypothesize that the presence of the more electron-withdrawing TFA ligand (compared to OAc) and HTFA may slow down the deactivation process, thus providing slightly more TOs in the first 4–8 hours.

Using the data discussed above and the identified reaction intermediates (see below), we propose reaction pathways for rhodium-catalyzed H/D exchange between toluene-d_8 and HOAc (Scheme 5). Under the acidic reaction conditions, the first step in the catalyzed H/D exchange reaction is likely oxidative addition of HOAc to (^{R}PNP)Rh(X) (X = TFA or OAc) to form (^{R}PNP)Rh(H)(X)$_2$ (**4**-**6**). The Rh^{III}–H intermediates can potentially catalyze H/D exchange to give an approximate 2:1 *meta*/*para* ratio as shown in Path A of Scheme 5. Here, we anticipate the possibility of cationic intermediates of the type [(^{R}PNP)Rh(H)(X)(toluene)][X] as precursors to arene C–D(H) bond breaking. In the presence of oxidant, either Cu(OAc)$_2$ or AgOAc, complexes (^{R}PNP)Rh(H)(X)$_2$ (**4**-**6**) can react to form HOAc and (^{R}PNP)Rh(X)$_3$ (**7**-**9**), which could also be active for arene C–D(H) bond breaking. Upon heating the reaction solution of (^{R}PNP)Rh(H)(X)$_2$ and (^{R}PNP)Rh(X)$_3$ mixture to 150 °C for ~1 h, complexes [(^{R}PNP)Rh(CO)][X] (**10**-**12**) were observed and existed during the H/D exchange reaction of toluene-d_8 with HOAc. Thus, we hypothesize that complexes **10**-**12** are possible catalysts for H/D exchange reactions that give an approximate 1:1 *meta*/*para* ratio (Path B, Scheme 5). Decomposition can also lead to insoluble and inactive Rh(s) species (Path C, Scheme 5), and the redissolution of this Rh species under oxidizing conditions could lead to a new Rh catalyst without the PNP ligand that catalyzes relatively slow H/D exchange. In our proposed reaction scheme, the relatively fast H/D exchange rate in the first 4–8 hours may be attributed to mixed mechanisms including Path A and pathways catalyzed by other (^{R}PNP)Rh^{III} species generated during the catalyst transformation, and the later decrease in rate can be explained by the disappearance of the active (^{R}PNP)Rh^{III} species **4**-**9** and the competing rate of the reverse D/H exchange.

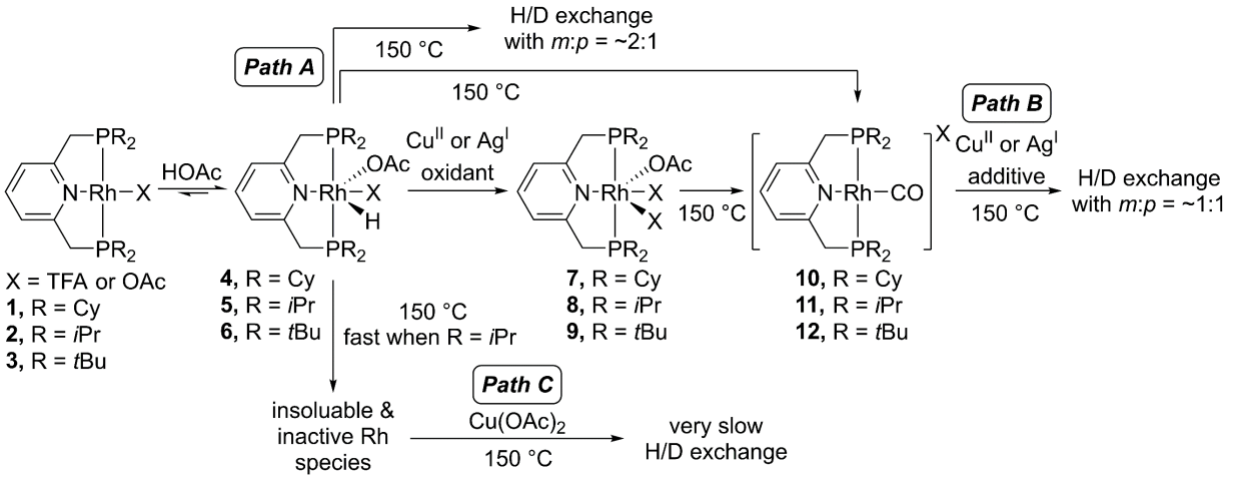

Scheme 5. Proposed pathways for Rh catalyzed H/D exchange of toluene-d_8 with HOAc.

Mechanistic Studies. To further understand the *meta*-selective catalytic H/D exchange results, *in situ* ^{31}P NMR spectroscopy studies were undertaken using similar reaction conditions to catalysis but with increased Rh concentration (0.4 mol% relative to toluene-d_8) and the same amount of $Cu(OAc)_2$ (Figure 7, left). After adding HOAc to a solution of (^{Cy}PNP)Rh(TFA) (**1a**) in toluene-d_8, a color change from dark-red to light-yellow was observed (see Figure S11), which is an indication of likely oxidation of Rh^{I} to Rh^{III}. Corresponding $^{31}P\{^{1}H\}$ NMR spectra are shown in Figure 7a-b (left). Upon addition of HOAc to the solution of **1a** in toluene-d_8, broadening of the ^{31}P NMR peak is observed together with a downfield shift from 42 ppm for **1a** to 46 ppm for (^{Cy}PNP)Rh(H)(OAc)(X) (X = TFA or OAc, **4**). The peak broadening might be caused by the exchange of coordinated OAc with free HOAc or TFA ion. Based on these observations, our hypothesis is that oxidative addition of HOAc to complex **1a** occurs to form a Rh^{III}–H complex **4** (Scheme 5). To confirm the formation of the Rh^{III}–H complex, the experiment was reproduced using a higher concentration of **1a** (5 mol% relative to toluene-d_8) with excess HOAc. A broad upfield singlet was observed in the ^{1}H NMR spectrum at –17.5 ppm, which is in a reasonable range compared to published Rh^{III}–H chemical shifts,[85-87,103] but the expected splitting pattern due to

coupling with rhodium and phosphorus was not observed. This is likely indicative of rapid exchange of the Rh^{III}–H ligand with an external proton source such as HOAc. The complex (^{Cy}PNP)Rh(OAc) (**1b**) was also used for the *in situ* $^{31}P\{^{1}H\}$ NMR spectroscopy study to reduce the number of potential reaction intermediates (Figure 7a-b, right). As expected, in the $^{31}P\{^{1}H\}$ NMR spectrum a doublet at 47 ppm with $^{1}J_{Rh,P}$ = 104 Hz was observed for (^{Cy}PNP)Rh(H)$(OAc)_2$ (**4b**). However, the expected multiplet for the hydride was not observed in the ^{1}H NMR spectrum, which supports the rapid exchange of Rh^{III}–H ligand with an external proton source.

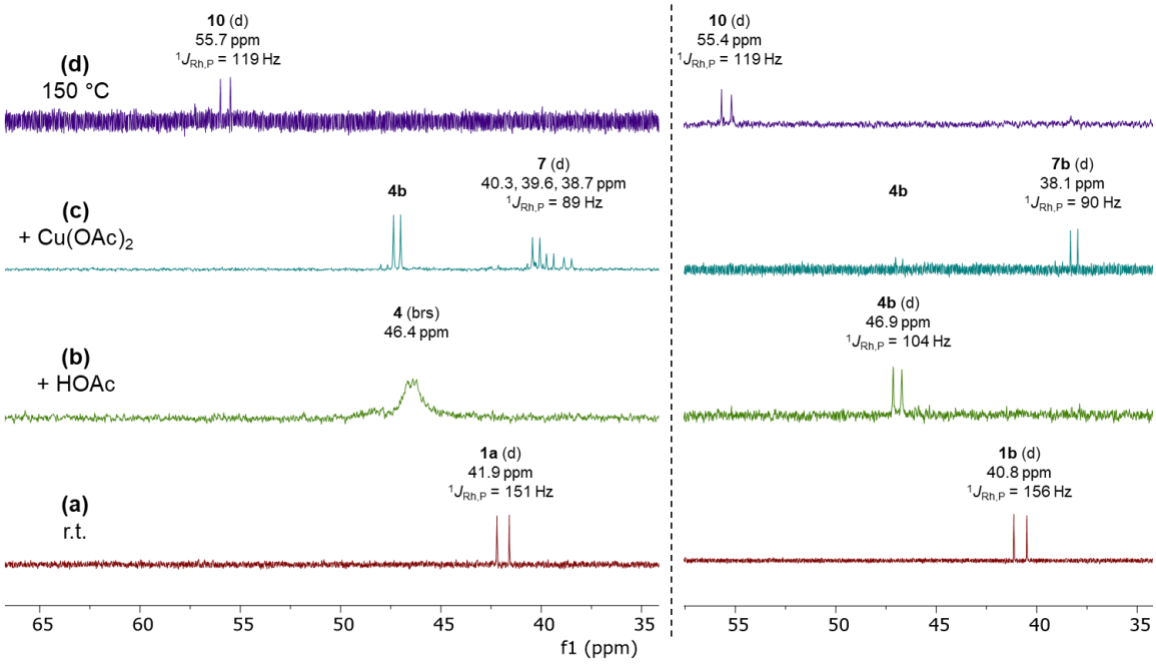

Figure 7. $^{31}P\{^{1}H\}$ NMR spectra of (^{Cy}PNP)Rh(X) (**1a-b**), $Cu(OAc)_2$, and HOAc in toluene-d_8. (a) Complex **1a** (left) in toluene-d_8, **1b** in benzene-d_6 (right). (b) After the addition of HOAc. (c) After the addition of $Cu(OAc)_2$ at 25 °C. (d) After heating to 150 °C.

Next, we attempted to isolate the putative Rh^{III}–H complex **4**. However, only a mixture of **1a** or **1b** and uncharacterized Rh^{III}–H complexes were obtained after drying the sample under vacuum. We assume that the oxidative addition of HOAc is reversible. Therefore, we attempted oxidative addition with a stronger acid, HTFA, to give an isolable Rh^{III}–H product (^{Cy}PNP)Rh(H)$(TFA)_2$ (**4a**). The ^{1}H and ^{31}P NMR spectra of **4a** showed similar peaks to complex **4**. A doublet of triplet

splitting pattern of Rh^{III}–H was observed in the ^{1}H NMR spectrum of **4a** (Figure 8a) demonstrating that **4a** does not undergo rapid exchange with free HTFA. The phosphorus–hydride coupling was confirmed in a $^{1}H\{^{31}P\}$ NMR spectrum, in which the doublet of triplet becomes a doublet (Figure 8a). By adjusting the ^{1}H-decoupler power and offset position in the $^{31}P\{^{1}H\}$ NMR, the hydride–phosphorus coupling could be observed separately from the methylene–phosphorus coupling, which gave almost the same $^{2}J_{H,P}$ as $^{2}J_{P,H}$ in the $^{1}H\{^{31}P\}$ NMR spectrum, which provided additional evidence for phosphorus–hydride coupling (Figure 8b).

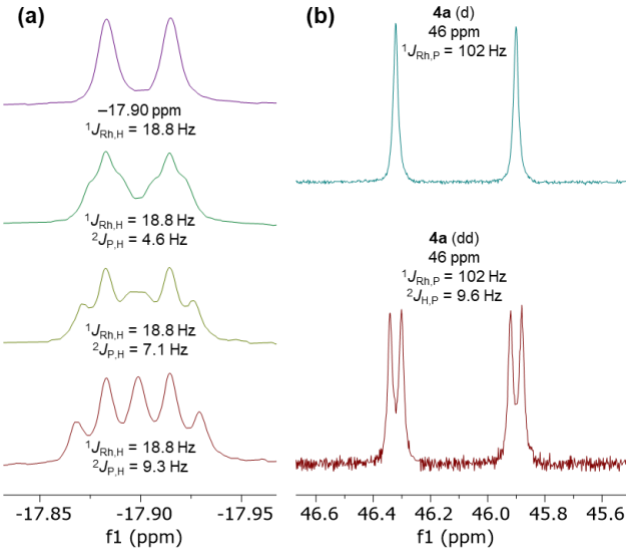

Figure 8. (a) ^{1}H NMR spectrum of the Rh^{III}–H peak of complex **4a** with different ^{31}P-decoupler powers (dpwr = 45, 35, 30 and 25 dB from top to bottom). (b) $^{31}P\{^{1}H\}$ NMR spectrum of **4a** with different ^{1}H-decoupler offsets {dof = −6000 Hz (top) and 0 Hz (bottom)} and powers (dpwr = 44 dB (top) and 38 dB (bottom)}.

In order to confirm that the Rh^{III}–H complexes **4** or **4a** are potential catalysts for H/D exchange, complex **4a** was tested for H/D exchange in the presence of $Cu(OAc)_2$ and compared to the exchange using **1a** (Figure 9). As expected, the exchange using **4a** gave almost identical TOs versus time plots to that using **1a** as the pre-catalyst, which supports the hypothesis that the pre-catalysts undergo oxidative addition of HOAc to generate Rh^{III}–H complexes that could potentially catalyze the H/D exchange reaction of toluene-d_8 with HOAc, and then convert to a second active

species in the later stage of the reaction. Also, a 1:1 *meta/para* ratio of H/D exchange using **4a** in the presence of $Cu(OAc)_2$ was observed, consistent with the *meta/para* ratio observed using **1a** as the pre-catalyst.

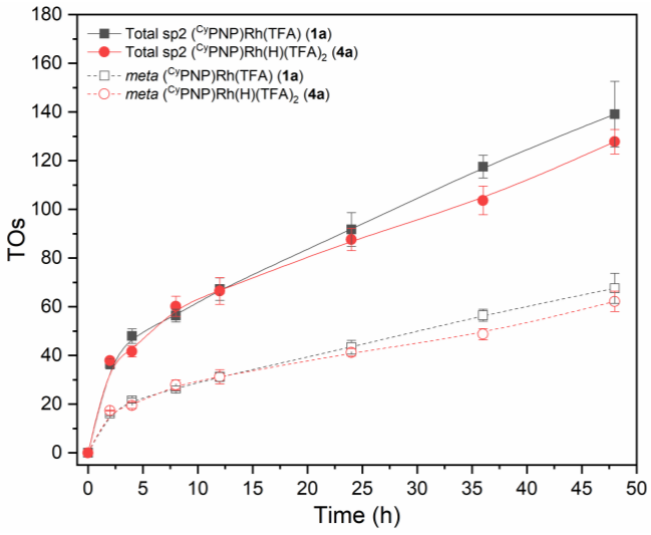

Figure 9. H/D exchange between toluene-d_8 and HOAc using (^{Cy}PNP)Rh(TFA) (**1a**) and (^{Cy}PNP)Rh(H)$(TFA)_2$ (**4a**) in the presence of $Cu(OAc)_2$ as the additive. Reaction conditions: toluene-d_8 (0.36 mL, 3.42 mmol), HOAc (0.64 mmol), Rh pre-catalyst (1.7 μmol), $Cu(OAc)_2$ (34 μmol), 150 °C, 30 psig N_2. Standard deviations are calculated from at least three independent experiments.

After the addition of $Cu(OAc)_2$ to (^{Cy}PNP)Rh(TFA) (**1a**), three new ^{31}P NMR peaks were observed with $^1J_{Rh,P} \sim 90$ Hz, which is commonly observed for Rh^{III} phosphine complexes (Figure 7c, left).[81-82] By using (^{Cy}PNP)Rh(OAc) (**1b**) as the starting reagent in the presence of HOAc, after addition of $Cu(OAc)_2$, only one intermediate (**7b**) was formed based on the ^{31}P{^{1}H} NMR spectrum (Figure 7c, right). Similarly, using **1b** with AgOAc and HOAc also results in the same intermediate **7b**, which contains two singlets in a 2:1 integration ratio (at 1.99 and 2.28 ppm) in the ^{1}H NMR spectrum that likely belong to the axial and equatorial OAc ligands (see Supporting information, Section 4.4). Based on these observations, we speculated that intermediate **7b** is likely to be (^{Cy}PNP)Rh$(OAc)_3$, and the three intermediates formed when using **1a** with HOAc and $Cu(OAc)_2$ are (^{Cy}PNP)Rh$(X)_3$ (X = TFA or OAc) (**7**). There is no observation of intermediate **7**

formation without $Cu(OAc)_2$ or AgOAc additives. Therefore, we hypothesize that during the H/D exchange reaction (^{R}PNP)Rh(H)$(X)_2$ (**4-6**) likely reacts with oxidant such as $Cu(OAc)_2$ or AgOAc to form (^{R}PNP)Rh$(X)_3$ (**7-9**). Aiming to understand the reactivity of (^{Cy}PNP)Rh$(X)_3$, the TOs of H/D exchange showing total sp^2 data and specific data for the *meta* position of toluene-d_8 using **1b** only and **1a** in the presence of $Cu(OAc)_2$ were plotted (Figure 10). Using **1b** without $Cu(OAc)_2$ would not lead to the formation of intermediate **7**. Using **1b** only and **1a** in the presence of $Cu(OAc)_2$ provided similar TOs(sp^2) but different TOs(*meta*) for the initial 4 hours. Without Cu^{II} additive the reaction stopped after 4 hours. Thus, the intermediate **7** is likely active for the H/D exchange of toluene-d_8 with HOAc and less selective for the *meta*-position compared to that using (^{R}PNP)Rh(H)$(OAc)_2$ (**4**, formed by **1b** with HOAc).

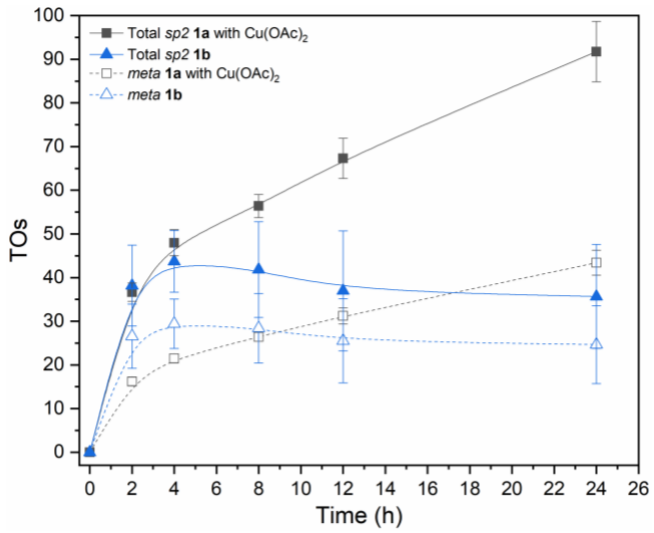

Figure 10. Comparison between H/D exchange between toluene-d_8 and HOAc using (^{Cy}PNP)Rh(TFA) (**1a**) in the presence of $Cu(OAc)_2$ and (^{Cy}PNP)Rh(OAc) (**1b**) only. Reaction conditions: toluene-d_8 (0.36 mL, 3.42 mmol), HOAc (0.64 mmol), Rh pre-catalyst (1.7 μmol), $Cu(OAc)_2$ (34 μmol), 150 °C, 30 psig N_2. Standard deviations are calculated from at least three independent experiments.

During the *in situ* ^{31}P NMR spectroscopy studies, all of the intermediates (**4** and **7**) appear to be converted to intermediate **10** (Figure 7d) with $^{1}J_{Rh,P}$ = 119 Hz after heating to 150 °C. To understand the identity of the unidentified intermediates **10-12** and the pathways for their

formation, different conditions were tested and monitored by NMR spectroscopy (Scheme 6). Based on these studies (see below), we propose that intermediates **10-12** are the carbonyl complexes [(^{R}PNP)Rh^{I}(CO)][X] (X = OAc or TFA). Monitoring the reaction of benzene-d_6 with HOAc by ^{1}H NMR and ^{31}P NMR spectroscopy using the different (^{R}PNP)Rh(X) complexes **1-3** shows the formation of intermediates **10-12** after heating at 150 °C in the presence of Cu(OAc)$_2$ or AgOAc. The intermediates **10-12** were also formed when heating the (^{R}PNP)Rh^{I} complexes **1-3** in HOAc/toluene-d_8 solution at 150 °C without the presence of Cu^{II} or Ag^{I} salt. This observation excludes the possibility of the intermediate being (^{R}PNP)Rh^{I}–M complexes (M = Cu or Ag), which could also have a similar $^{1}J_{Rh,P}$ of approximately 120 Hz and could be formed by heating the Rh^{I} complex in the presence of metal salts.[84,98,104] Also, heating the complexes **1-3** to 150 °C in toluene-d_8 did not result in the formation of **10-12**, but the intermediates **10-12** were observed when heating the Rh^{III}–H complexes **4-6** in toluene-d_8. The ^{13}C{^{1}H} NMR spectrum of the intermediate **10** reveals a doublet of triplets at 194.7 ppm ($^{1}J_{Rh,C}$ = 70 Hz, $^{2}J_{P,C}$ = 15 Hz) (Figure 11), and the reaction solution exhibits an IR absorption at 1985 cm^{-1}. These data are almost identical to the published examples of [(^{R}PNP)Rh^{I}(CO)]$^{+}$ complexes (R = isopropyl and *tert*-butyl).[81,87,105-106]

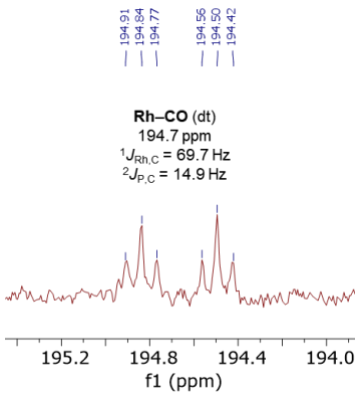

Figure 11. Resonance due to the CO ligand in the ^{13}C{^{1}H} NMR spectrum of [(^{Cy}PNP)Rh(CO)][X] (**10**) (X = OAc or TFA).

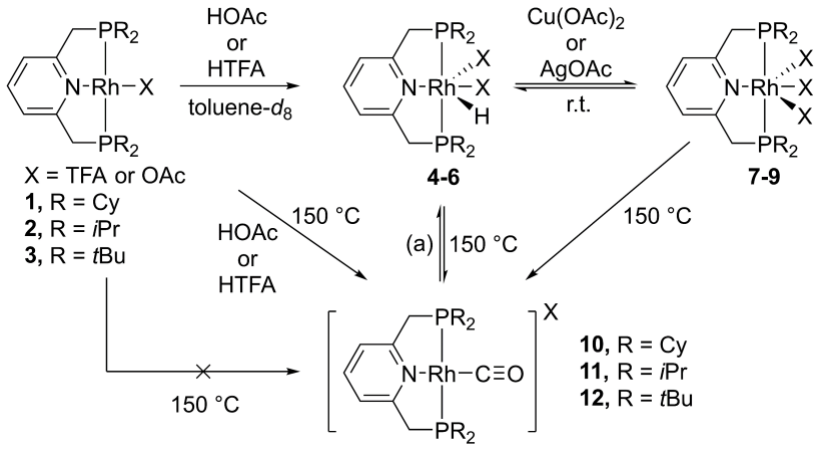

Scheme 6. Possible transformations during the H/D exchange. (a) Vacuum to dryness in the presence of excess HOAc or HTFA.

With the assumption that [(^{R}PNP)Rh^{I}(CO)][X] (X = OAc or TFA) (**10**-**12**) is a potential catalyst resting state for Rh-mediated H/D exchange of toluene-d_8 with HOAc, a catalytic cycle can be proposed for Path B of Scheme 5 (Scheme 7). Following oxidative addition of HOAc to [(^{R}PNP)Rh(CO)][X] (**10**-**12**), arene C–D(H) bond activation could occur to form a cationic [(^{R}PNP)Rh(CO)(H)(tolyl-d_7)][X] intermediate. Toluene-d_7 reductive elimination completes the H/D exchange and regenerates the catalysts **10**-**12**. The oxidative addition of the HOAc to [(^{R}PNP)Rh(CO)][X] (**10**-**12**) could be slower compared to the same reaction with (^{R}PNP)Rh(X), which could explain the decreased rate of H/D exchange rate in the later stages of the H/D exchange reactions where Rh is nearly completely converted to [(^{R}PNP)Rh(CO)][X]. Indeed, by adding HTFA to a solution of [($^{i\text{Pr}}$PNP)Rh(CO)][TFA] in benzene at room temperature, no formation of Rh–H was observed by ^{1}H NMR spectroscopy (only peak shifting was observed due to the change of solvent polarity).

The observed ligand effects can also be explained. Using [(^{R}PNP)Rh(CO)][X] with the bulky *tert*-butyl group (complex **12**) likely disfavors acetic acid oxidative addition (both sterically and electronically, as discussed above),[81,83,107] therefore, resulting in the slower H/D exchange rate

compared to that with a less bulky cyclohexyl group (e.g., complex **10**). The presence of Cu^{II} or Ag^{I} additive could facilitate oxidative addition of HOAc, by an unknown mechanism, as well as stabilizing the Rh–H intermediates from decomposition to inactive Rh(s).

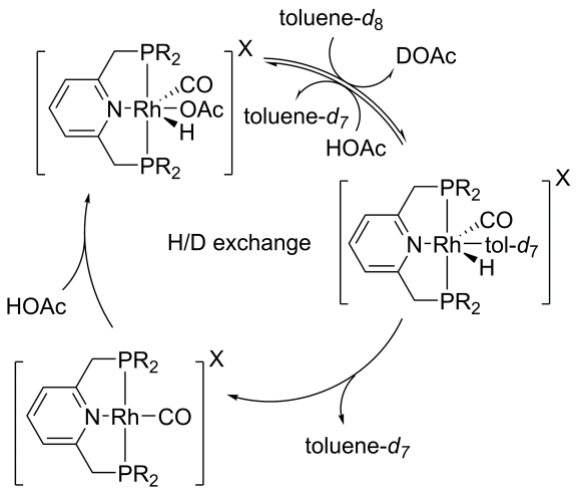

Scheme 7. Proposed catalytic cycle for Path B (Scheme 5) of Rh catalyzed H/D exchange of toluene-d_8 with HOAc.

Rh catalyzed decarbonylation of aldehydes has been reported;[108-112] however, decarbonylation of carboxylate to generate a Rh–CO complex is uncommon. In addition, during the H/D exchange reaction, the formation of Rh–OR or HOR (R = CF_3 or CH_3) compounds, which are possible intermediates during carboxylate decarbonylation, was not observed. Instead, HCF_3 was observed as a product during the conversion of the Rh–H complex **7** to the Rh–CO complex **10** using NMR spectroscopy (^{1}H NMR, 5.34 ppm, quartet, $^2J_{F,H}$ = 79 Hz; ^{19}F NMR, –76.1 ppm, doublet, $^2J_{H,F}$ = 79 Hz). It is possible that CO is formed by the thermal decomposition of formic acid, which could be generated during the catalysis, and then captured by the (^{R}PNP)Rh intermediate to produce the observed [(^{R}PNP)Rh(CO)][X] complex. However, based on the current experimental evidence, pathways for the formation of formic acid are not elucidated. Also, we speculate on another potential reaction pathway for the formation of [(^{R}PNP)Rh(CO)][X] (Scheme 8) with the following explanations: (1) The decarboxylation of (^{R}PNP)Rh(OC(O)CF_3) seems to be a more reasonable

reaction pathway to form the (^{R}PNP)Rh(CF_3) species and CO_2 during the thermolysis since this process has been reported for Rh carboxylate complexes.[113-114] (2) Complexes of the type (^{R}PNP)Rh(H) are known as catalysts for activation of CO_2 at room temperature with the ultimate formation of [(^{R}PNP)Rh(CO)][X] under acidic conditions.[105] Although PhTFA was not observed during the conversion, it is likely because the trifluoroacetate served as a pseudo-halide and lead to a rapid consumption of PhTFA by oxidative addition to (^{R}PNP)Rh(X). The observation of deuterium incorporation at the ^{R}PNP methylene position is consistent with the potential formation of ligand dearomatized intermediates. However, based on the current data, we cannot eliminate other possible reaction pathways for the formation of [(^{R}PNP)Rh(CO)][X] (see Supporting information, Section 4.8).

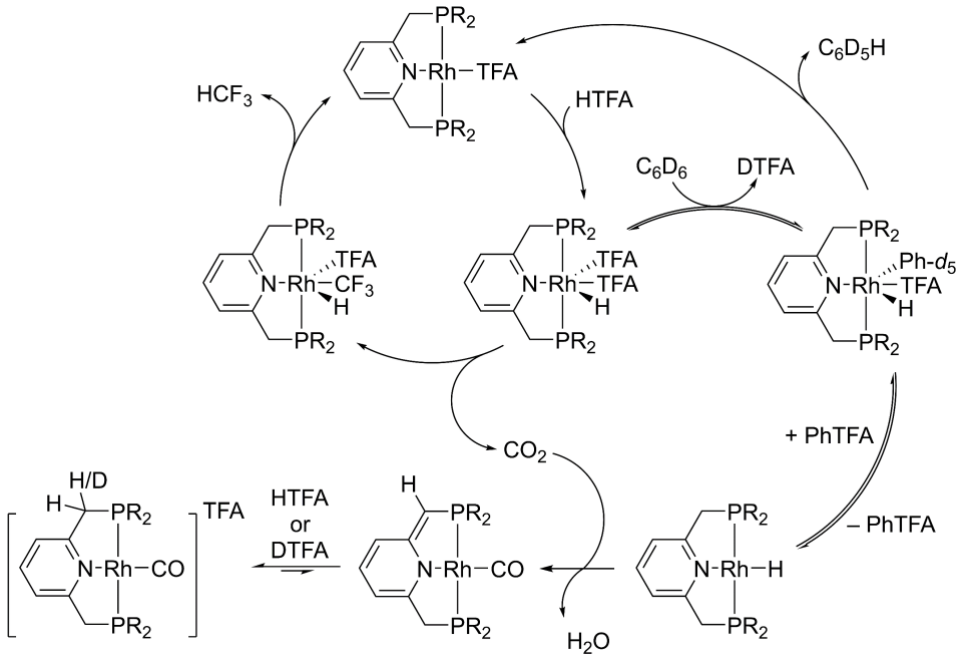

Scheme 8. Speculated pathway for the formation of [(^{R}PNP)Rh(CO)][X] (**10-12**).

Conclusions

The (^{R}PNP)Rh complexes offer advantages for C–H activation of arenes; however, in some cases the homogeneous Rh catalysts undergo rapid deactivation to form Rh(s) in weak acids at

high reaction temperature (150 °C). Thus, the development of strategies to stabilize ligated Rh catalysts, facilitating Rh-mediated C–H activation processes, and understanding the conversion of the Rh species are important for future ligand design and optimization for the catalytic processes. Here, a series of (^{R}PNP)Rh carboxylate complexes have been used to study catalytic H/D exchange between toluene-d_8 and acetic acid in order to better understand the catalyst conversion, ligand effect, and screening for additives with positive effects. Several reaction intermediates were identified and [(^{R}PNP)Rh^{I}(CO)][X] was found to be an observable catalyst resting state during the late stages of the Rh-mediated catalytic H/D exchange.

Various of the Lewis acidic additives have been examined and have been demonstrated to exhibit different functions. Typical strong Lewis acids serve as catalysts themselves for H/D exchange via $^{Ar}S_E$ mechanism, while weaker non-oxidizing Lewis additive facilitate the Rh-mediated C–H(D) activation of toluene but are unable to prevent the (^{R}PNP)Rh catalysts from rapid decomposition to form Rh(s). Additives such as $Cu(OAc)_2$ and AgOAc were found to facilitate the (^{R}PNP)Rh catalyzed H/D exchange by facilitating the conversion of the pre-catalyst to the active species, potentially facilitating the oxidative addition process of HOAc, and stabilizing the active (^{R}PNP)Rh species from decomposition to inactive Rh(s).

Experimental Section

General information. All reactions were performed under a dinitrogen atmosphere using Schlenk line techniques or inside a dinitrogen filled glovebox unless specified otherwise. All NMR reactions were performed using Wilmad medium wall precision low pressure/vacuum (LPV) NMR tube and pressurized with dinitrogen using a high-pressure line. Tetrahydrofuran and diethyl ether were dried via potassium-benzophenone/ketyl stills under dinitrogen atmosphere and stored over

activated 4 Å molecular sieves inside the glovebox. Methanol was dried via a calcium hydride still under dinitrogen atmosphere and stored inside a glovebox. Benzene and methylene chloride were dried using a solvent purification system with activated alumina and stored under activated 3 Å molecular sieves inside the dinitrogen fumed glovebox. Toluene-d_8, acetonitrile-d_3, benzene-d_6, and methylene chloride-d_2 were dried and stored over activated 3 Å molecular sieves inside a glovebox. All other chemicals were purchased from commercial sources and used as received. NMR spectra were recorded on Varian VNMRS 600 MHz or 500 MHz spectrometer or a Bruker Avance III 800 MHz spectrometer. All reported chemical shifts were referenced to residual ^{1}H resonances (^{1}H NMR) or ^{13}C{^{1}H} resonances (^{13}C{^{1}H} NMR). ^{1}H NMR: acetonitrile-d_3 1.94 ppm; benzene-d_6 7.16 ppm; chloroform-d 7.26 ppm; dimethyl sulfoxide-d_6 2.50 ppm; methylene chloride-d_2 5.32 ppm; toluene-d_8 7.09 ppm. ^{13}C NMR: acetonitrile-d_3 1.3 ppm, 118.3 ppm; benzene-d_6 128.1 ppm; chloroform-d 77.2 ppm; dimethyl sulfoxide-d_6 39.5 ppm; methylene chloride-d_2 53.8 ppm; toluene-d_8 137.5 ppm.[115] ^{19}F NMR spectra were referenced to hexafluorobenzene δ –164.9 ppm using an external standard. ^{31}P NMR spectra were referenced to H_3PO_4 δ 0.0 ppm using an external standard. Infrared spectra were obtained using a thin film method with a NaCl salt plate using a Shimadzu IRAffinity-1 FT-IR spectrophotometer. Elemental analyses were performed by Midwest Microlab, Indianapolis, Indiana. or the UVA Chemistry Department, Charlottesville, Virginia.

***In Situ* ^{1}H NMR Studies of H/D Exchange of Toluene-d_8 with HOAc.** Described here is a representative procedure for our NMR studies of catalytic H/D exchange. Under an atmosphere of dry dinitrogen, the additive (34 μmol, 20 equiv. relative to Rh pre-catalyst) was charged into at least three medium-wall LPV NMR tubes. A stock solution of Rh pre-catalyst (14 μmol, 0.05 mol% relative to toluene-d_8) in toluene-d_8 (3 mL, 28 mmol) was made to ensure reproducible

concentration of Rh complex. Then, HOAc (300 μL, 5 mmol) was added to the stock solution. After stirring the solution color changed from dark red to light-yellow. Next, 400 μL of the stock solution (toluene-d_8 3.42 mmol, HOAc 0.64 mmol, Rh pre-catalyst 1.7 μmol) was added via syringe into each LPV NMR tube. The LPV NMR tubes were pressurized with 30 psig of dinitrogen. The quantitative ^{1}H NMR experiments were performed using a sealed capillary tube filled with $MeNO_2$/$MeNO_2$-d_3 as standard. The LPV NMR tube was heated in an oil bath at a specific temperature, then the integration changes of toluene *ortho*-, *meta*-, and *para*-protons and the toluene methyl signal were measured at time intervals by ^{1}H NMR experiments. In order to obtain more accurate integration in the ^{1}H NMR spectrum, the relaxation delay time (d_1) was set to 30 s. The turnovers (TOs) of *ortho*-, *meta*-, and *para*- H/D exchange were calculated based on the integration change of *ortho*-, *meta*-, and *para*-proton peaks compared to the reference peak in the ^{1}H NMR spectra. Standard deviations are calculated from at least three independent experiments.

Synthesis and Characterization of Rh complexes. (^{Cy}PNP)Rh(TFA) (1a). To a solution of [Rh(η^2-C_2H_4)$_2$(μ-TFA)]$_2$ (50 mg, 0.092 mmol) in 20 mL THF, ^{Cy}PNP (92 mg, 0.184 mmol) was added. After stirring for 4 h, the mixture was dried under vacuum to yield an orange-red solid. The crude product was purified via recrystallization from THF and *n*-pentane to yield a red solid product (102 mg, 77% isolated yield). ^{1}H NMR (600 MHz, benzene-d_6) δ 6.85 (t, $^3J_{H,H}$ = 8 Hz, 1H, py 4-*H*), 6.32 (d, $^3J_{H,H}$ = 8 Hz, 2H, py 3,5-*H*), 2.57 (br s, 4H, PC*H*$_2$), 2.48 (d, *J* = 12 Hz, 4H), 2.02 (p vt, $^3J_{H,H}$ = 3 Hz, *J* = 13 Hz, 4H, Cy C*H*), 1.77 (d, *J* = 13 Hz, 4H), 1.71 – 1.62 (m, 8H), 1.60 – 1.49 (m, 12H), 1.32 – 1.24 (m, 4H), 1.21 – 1.13 (m, 8H). ^{19}F NMR (564 MHz, benzene-d_6) δ –72.1. ^{31}P{^{1}H} NMR (243 MHz, benzene-d_6) δ 41.9 (d, $^1J_{Rh,P}$ = 151 Hz). ^{13}C{^{1}H} NMR (201 MHz, benzene-d_6) δ 165.0 (vt, py *C*-2,6), 161.9 (q, $^2J_{F,C}$ = 35 Hz, *C*(O)CF_3), 130.2 (s, py *C*-4), 119.7 (vt,

py *C*-3,5), 116.4 (q, $^{1}J_{F,C}$ = 290 Hz, C(O)*C*F$_3$), 35.4 (vt, P*C*H$_2$), 34.4 (vt, Cy *C*H), 29.4, 28.6, 27.3 (vt), 27.2 (vt), 26.7. Anal. Calcd for $C_{33}H_{51}F_3NO_2P_2Rh$: C, 55.39; H, 7.18; N, 1.96. Found: C, 54.90; H, 7.29; N, 1.85.

(^{Cy}PNP)Rh(OAc) (1b). To a solution of ^{Cy}PNP (115 mg, 0.230 mmol) in 20 mL THF or Et$_2$O, [Rh(η^2-C$_2$H$_4$)$_2$(μ-OAc)]$_2$ (50 mg, 0.116 mmol) was added. After stirring for 4 h, the mixture was filtered through Celite. The filtrate was dried under vacuum to yield a dark-red solid product (98 mg, 65% isolated yield). ^{1}H NMR (600 MHz, benzene-*d*$_6$) δ 6.92 (t, $^{3}J_{H,H}$ = 8 Hz, 1H, py 4-*H*), 6.36 (d, $^{3}J_{H,H}$ = 8 Hz, 2H, py 3,5-*H*), 2.60 (vt, *J* = 4 Hz, 4H, PC*H*$_2$), 2.57 (d, *J* = 13 Hz, 4H), 2.33 (s, 3H, C(O)C*H*$_3$), 2.14 (p vt, $^{3}J_{H,H}$ = 3 Hz, *J* = 13 Hz, 4H, Cy C*H*), 1.84 – 1.69 (m, 12H), 1.68 – 1.56 (m, 12H), 1.36 – 1.27 (m, 4H), 1.24 – 1.17 (m, 8H). ^{31}P{^{1}H} NMR (243 MHz, benzene-*d*$_6$) δ 40.8 (d, $^{1}J_{Rh,P}$ = 156 Hz). ^{13}C{^{1}H} NMR (201 MHz, benzene-*d*$_6$) δ 175.1 (s, *C*(O)CH$_3$), 164.5 (vt, py *C*-2,6), 128.9 (s, py *C*-4), 119.5 (vt, py *C*-3,5), 35.9 (vt, P*C*H$_2$), 34.7 (vt, Cy *C*H), 29.6 (vt), 28.7, 27.6 (vt), 27.4 (vt), 26.9, 24.1 (s, C(O)*C*H$_3$). We were unable to obtain clean elemental analysis data, representative NMR spectra are provided in the Supporting Information.

($^{i\text{Pr}}$PNP)Rh(TFA) (2a). To a solution of $^{i\text{Pr}}$PNP (125 mg, 0.368 mmol) in 25 mL THF, [Rh(η^2-C$_2$H$_4$)$_2$(μ-TFA)]$_2$ (100 mg, 0.184 mmol) was added. After stirring for at least 1 h, the mixture was filtered through Celite. The filtrate was dried under vacuum and then washed with *n*-pentane to obtain a red solid. The crude product was purified by recrystallization from THF and *n*-pentane at -35 °C to yield a red solid that was comprised of needle shaped crystals (172 mg, 84% isolated yield). ^{1}H NMR (600 MHz, benzene-*d*$_6$) δ 6.82 (t, $^{3}J_{H,H}$ = 8 Hz, 1H, py 4-*H*), 6.26 (d, $^{3}J_{H,H}$ = 8 Hz, 2H, py 3,5-*H*), 2.41 (vt, *J* = 4 Hz, 4H, PC*H*$_2$), 2.05 (hept vt, $^{3}J_{H,H}$ = 7 Hz, *J* = 2 Hz, 4H, C*H*(CH$_3$)$_2$), 1.37 (d vt, $^{3}J_{H,H}$ = 9 Hz, *J* = 7 Hz, 12H, CH(C*H*$_3$)$_2$), 1.01 (d vt, $^{3}J_{H,H}$ = 7 Hz, *J* = 7 Hz, 12H, CH(C*H*$_3$)$_2$). ^{19}F NMR (564 MHz, benzene-*d*$_6$) δ –72.1. ^{31}P{^{1}H} NMR (243 MHz, Benzene-*d*$_6$) δ

49.3 (d, $^{1}J_{Rh,P}$ = 151 Hz). $^{13}C\{^{1}H\}$ NMR (201 MHz, benzene-d_6) δ 164.8 (vt, py *C*-2,6), 161.9 (q, $^{2}J_{F,C}$ = 34 Hz, *C*(O)CF_3), 130.4 (s, py *C*-4), 119.8 (vt, py *C*-3,5), 116.3 (q, $^{1}J_{F,C}$ = 293 Hz, C(O)*C*F_3), 34.9 (vt, P*C*H_2), 24.8 (vt, *C*H$(CH_3)_2$), 19.3 (vt, CH(*C*$H_3)_2$), 18.0 (s, CH(*C*$H_3)_2$). Anal. Calcd for $C_{21}H_{35}F_3NO_2P_2Rh$: C, 45.42; H, 6.35; N, 2.52. Found: C, 45.40; H, 6.43; N, 2.63.

($^{i\text{Pr}}$PNP)Rh(OAc) (2b). To a solution of $^{i\text{Pr}}$PNP (78 mg, 0.230 mmol) in 20 mL THF or Et_2O, a solution of $[Rh(\eta^2\text{-}C_2H_4)_2(\mu\text{-}OAc)]_2$ (50 mg, 0.116 mmol) in 20 mL of THF or Et_2O was added dropwise. After stirring for 0.5 h, the mixture was filtered through Celite. The filtrate was dried under vacuum to obtain a red sticky oil. The crude oil product was redissolved in a minimal amount of dry Et_2O, and cold *n*-pentane was added slowly. The precipitate, a dark red solid, was collected by filtration (58 mg, 50% isolated yield). ^{1}H NMR (600 MHz, benzene-d_6) δ 6.87 (t, $^{3}J_{H,H}$ = 8 Hz, 1H, py 4-*H*), 6.27 (d, $^{3}J_{H,H}$ = 8 Hz, 2H, py 3,5-*H*), 2.46 (vt, *J* = 4 Hz, 4H, PCH_2), 2.30 (s, 3H, C(O)CH_3), 2.21 (hept vt, $^{3}J_{H,H}$ = 7 Hz, *J* = 2 Hz, 4H, C*H*$(CH_3)_2$), 1.46 (d vt, $^{3}J_{H,H}$ = 8 Hz, *J* = 7 Hz, 12H, CH(C$H_3)_2$), 1.11 (d vt, $^{3}J_{H,H}$ = 7 Hz, *J* = 7 Hz, 12H, CH(C$H_3)_2$). ^{31}P NMR (243 MHz, benzene-d_6) δ 48.10 (d, $^{1}J_{Rh,P}$ = 157 Hz). $^{13}C\{^{1}H\}$ NMR (201 MHz, benzene-d_6) δ 175.2 (s, *C*(O)CH_3), 164.4 (vt, py *C*-2,6), 128.9 (s, py *C*-4), 119.6 (vt, py *C*-3,5), 35.4 (vt, P*C*H_2), 25.0 (vt, *C*H$(CH_3)_2$), 24.0 (s, C(O)*C*H_3), 19.6 (vt, CH(*C*$H_3)_2$), 18.2 (s, CH(*C*$H_3)_2$). We were unable to obtain clean elemental analysis data, representative NMR spectra are provided in the Supporting Information.

(^{Cy}PNP)Rh(H)(TFA)$_2$ (4a). To a solution of **1a** (100 mg, 0.140 mmol) in 20 mL benzene, HTFA (20 μL, 0.280 mmol) was added. The color of the solution changed to light yellow immediately. After stirring for 10 min, the mixture was dried under vacuum to yield a yellow solid. Then, the crude product was recrystallized from THF and *n*-pentane to yield a light-yellow solid, which was dried *in vacuo* and collected (106 mg, 80% isolated yield). ^{1}H NMR (600 MHz, benzene-d_6) δ 14.97 (br s, 1H, *H*TFA), 6.73 (t, $^{3}J_{H,H}$ = 8 Hz, 1H, py 4-*H*), 6.39 (d, $^{3}J_{H,H}$ = 8 Hz,

2H, py 3,5-*H*), 3.48 (d vt, $^{2}J_{H,H}$ = 17 Hz, J = 4 Hz, 2H, PCH_2), 2.69 (d vt, $^{2}J_{H,H}$ = 17 Hz, J = 4 Hz, 2H, PCH_2), 2.46 (p vt, $^{3}J_{H,H}$ = 3 Hz, J = 13 Hz, 2H, Cy C*H*), 2.22 (d, J = 13 Hz, 2H), 2.10 (d, J = 13 Hz, 2H), 2.03 (d, J = 13 Hz, 2H), 1.98 (vt, J = 12 Hz, 2H, Cy C*H*), 1.77 (s, 4H), 1.67 (s, 2H), 1.57 (d, 4H), 1.55 – 1.41 (m, 8H), 1.38 – 1.21 (m, 8H), 1.19 – 1.04 (m, 8H), –17.81 (d vt, $^{1}J_{Rh,H}$ = 19 Hz, J = 10 Hz, 1H, Rh–*H*). ^{19}F NMR (564 MHz, benzene-d_6) δ –71.9 (s, 3F), –73.5 (br d, 6F, due to exchange). ^{31}P{^{1}H} NMR (243 MHz, benzene-d_6) δ 46.1 (dd, $^{1}J_{Rh,P}$ = 102 Hz, $^{2}J_{H,P}$ = 10 Hz). ^{13}C{^{1}H} NMR (201 MHz, benzene-d_6) δ 165.7 (vt, py *C*-2,6), 162.7 (q, $^{2}J_{F,C}$ = 36 Hz, *C*(O)CF_3), 137.1 (s, py *C*-4), 120.7 (vt, py *C*-3,5), 115.3 (q, $^{1}J_{F,C}$ = 291 Hz, C(O)*C*F_3), 36.6 (vt, Cy *C*H), 36.3 (vt, Cy *C*H), 35.3 (vt, P*C*H_2), 29.2, 28.8, 28.4, 28.2, 27.5 (dt, two overlapping vt peaks), 27.1 (q, two overlapping vt peaks), 26.4, 26.3. The *C*(O)*C*F_3 resonances were buried in the baseline due to the exchange with free HTFA. Anal. Calcd for $C_{35}H_{52}F_6NO_4P_2Rh$·1.0 HTFA: C, 47.09; H, 5.66; N, 1.48. Found: C, 47.02; H, 5.71; N, 1.48.

(*i*^{Pr}PNP)Rh(H)(TFA)$_2$ (5a). Using the same procedure as for **4a** with **2a** (50 mg, 0.090 mmol) and HTFA (20 μL, 0.280 mmol) in 10 mL of benzene to give a light yellow solid product (42 mg, 70% isolated yield). ^{1}H NMR (600 MHz, benzene-d_6) δ 10.94 (br s, 1.5H, *H*TFA), 6.65 (t, $^{3}J_{H,H}$ = 8 Hz, 1H, py 4-*H*), 6.29 (d, $^{3}J_{H,H}$ = 8 Hz, 2H, py 3,5-*H*), 3.37 (d vt, $^{2}J_{H,H}$ = 18 Hz, J = 4 Hz, 2H, PCH_2), 2.49 (d vt, $^{2}J_{H,H}$ = 18 Hz, J = 4 Hz, 2H, PCH_2), 2.40 (hept vt, $^{3}J_{H,H}$ = 7 Hz, J = 3 Hz, 2H, C*H*(CH_3)$_2$), 1.97 – 1.86 (m, 2H, C*H*(CH_3)$_2$), 1.14 (d vt, $^{3}J_{H,H}$ = 8 Hz, J = 8 Hz, 12H, two overlapping d vt peaks, CH(C*H*$_3$)$_2$), 1.05 (d vt, $^{3}J_{H,H}$ = 9 Hz, J = 7 Hz, 6H, CH(C*H*$_3$)$_2$), 0.68 (d vt, $^{3}J_{H,H}$ = 8 Hz, J = 7 Hz, 6H, CH(C*H*$_3$)$_2$), –17.97 (d vt, $^{1}J_{Rh,H}$ = 20 Hz, J = 11 Hz, 1H, Rh–*H*). ^{19}F NMR (564 MHz, benzene-d_6) δ –72.1 (s, 3F), –74.0 (br s, 7.5F, due to exchange). ^{31}P{^{1}H} NMR (243 MHz, benzene-d_6) δ 53.9 (dd, $^{1}J_{Rh,P}$ = 103 Hz, $^{2}J_{H,P}$ = 9 Hz). ^{13}C NMR (201 MHz, benzene-d_6) δ 165.5 (vt, py *C*-2,6), 163.8 (q, $^{2}J_{F,C}$ = 37 Hz, *C*(O)CF_3), 137.4 (s, py *C*-4), 121.0 (vt, py *C*-

3,5), 116.0 (q, $^{1}J_{F,C}$ = 288 Hz, C(O)*C*F_3), 114.5 (q, $^{1}J_{F,C}$ = 290 Hz, C(O)*C*F_3), 36.1 (vt, P*C*H_2), 26.3 (vt, *C*H(CH_3)$_2$), 25.2 (vt, *C*H(CH_3)$_2$), 18.7 (s, CH(*C*H_3)$_2$), 18.3 (s, CH(*C*H_3)$_2$), 17.8 (s, CH(*C*H_3)$_2$), 17.3 (s, CH(*C*H_3)$_2$). One of the *C*(O)CF_3 resonances was buried in the baseline due to the exchange with free HTFA. Anal. Calcd for $C_{23}H_{36}F_6NO_4P_2Rh$·1.5 HTFA: C, 37.16; H, 4.50; N, 1.67. Found: C, 37.59; H, 4.55; N, 1.69. Anal. Calcd for $C_{23}H_{36}F_6NO_4P_2Rh$·1.6 HTFA: C, 36.94; H, 4.45; N, 1.64. Found: C, 36.55; H, 4.26; N, 1.58. The amount of HTFA was quantified using ^{1}H NMR spectroscopy of the analysis sample. Samples with different amount of remaining HTFA were sent for EA to confirm the analysis results.

(*t*^{Bu}PNP)Rh(H)(TFA)$_2$ (6a). Using the same procedure as for **4a** with **3a** (100 mg, 0.164 mmol) and HTFA 20 (30 μL, 0.392 mmol) in 20 mL of benzene to give a light yellow solid product (110 mg, 80% isolated yield). ^{1}H NMR (800 MHz, benzene-d_6) δ 14.72 (br s, 0.9H, *H*TFA), 6.73 (t, $^{3}J_{H,H}$ = 8 Hz, 1H, py 4-*H*), 6.35 (d, $^{3}J_{H,H}$ = 8 Hz, 2H, py 3,5-*H*), 3.59 (br s, 2H, PCH_2), 2.68 (d, $^{2}J_{H,H}$ = 17 Hz, 2H, PCH_2), 1.21 (br s, 18H, C(CH_3)$_3$), 1.06 (br s, 18H, C(CH_3)$_3$), –17.77 (br s, 1H, Rh–*H*). ^{19}F NMR (564 MHz, benzene-d_6) δ –72.3 (s, 3F), –73.8 (br s, 5.7F). ^{31}P NMR (243 MHz, benzene-d_6) δ 68.9 (dd, $^{1}J_{Rh,P}$ = 103 Hz, $^{2}J_{H,P}$ = 13 Hz). ^{13}C{^{1}H} NMR (201 MHz, benzene-d_6) δ 166.3 (s, py *C*-2,6), 162.6 (q, $^{2}J_{F,C}$ = 36 Hz, *C*(O)CF_3), 161.5 (q, $^{2}J_{F,C}$ = 35 Hz, *C*(O)CF_3), 137.7 (s, py *C*-4), 120.6 (s, py *C*-3,5), 115.2 (q, $^{1}J_{F,C}$ = 288 Hz, C(O)*C*F_3), 36.2 (s, *C*(CH_3)$_3$), 35.8 (vt, P*C*H_2), 35.6 (s, *C*(CH_3)$_3$), 29.2 (s, C(*C*H_3)$_3$), 28.8 (s, C(*C*H_3)$_3$). One of the *C*F_3 resonances was buried in the baseline due to the exchange with free HTFA. ^{1}H NMR (497 MHz, toluene-d_8, 213 K) δ 15.86 (s, 0.9H, *H*TFA), 6.68 (t, $^{3}J_{H,H}$ = 8 Hz, 1H, py 4-*H*), 6.29 (d, $^{3}J_{H,H}$ = 8 Hz, 2H, py 4-*H*), 3.37 (d, $^{2}J_{H,H}$ = 18 Hz, 2H, PCH_2), 2.45 (d, $^{2}J_{H,H}$ = 18 Hz, 2H, PCH_2), 1.05 (vt, *J* = 7 Hz, 18H, C(CH_3)$_3$), 0.98 – 0.87 (vt, *J* = 6 Hz, 18H, C(CH_3)$_3$), –18.01 (d vt, $^{1}J_{Rh,H}$ = 12 Hz, *J* = 7 Hz, 1H, Rh–*H*). ^{19}F NMR (564 MHz, toluene-d_8) δ –72.35 (s, 3F), –74.02 (br s, 5.7F). ^{31}P NMR (243 MHz, toluene-

d_8) δ 68.82 (d, $^1J_{Rh,P}$ = 100 Hz). Anal. Calcd for $C_{27}H_{44}F_6NO_4P_2Rh$·0.9 HTFA: C, 41.77; H, 5.47; N, 1.69. Found: C, 41.91; H, 5.36; N, 1.49. The amount of remaining HTFA was calculated based on the integration in the ^{1}H NMR and ^{19}F NMR of the sample that was sent for elemental analysis.

Associated Content

Supporting Information

The Supporting Information is available free of charge.

Additional experimental details, NMR spectra of the complexes and intermediates, IR spectra and crystal structure data (PDF).

Access Codes

CCDC 2032719–2032724 contain the supplementary crystallographic data for this paper. These data can be obtained free of charge via www.ccdc.cam.ac.uk/structures.

Author Information

Corresponding Author

T. Brent Gunnoe − Department of Chemistry, University of Virginia, Charlottesville, Virginia 22904, United States; orcid.org/0000-0001-5714-3887; Email: tbg7h@virginia.edu

Authors

Fanji Kong − Department of Chemistry, University of Virginia, Charlottesville, Virginia 22904, United States; orcid.org/0000-0003-4136-1403

Shunyan Gu − Department of Chemistry, University of Virginia, Charlottesville, Virginia 22904, United States; orcid.org/0000-0002-3625-1042

Chang Liu − Department of Chemistry, University of Virginia, Charlottesville, Virginia 22904, United States; orcid.org/0000-0002-7568-0608

Diane A. Dickie − Department of Chemistry, University of Virginia, Charlottesville, Virginia 22904, United States; orcid.org/0000-0003-0939-3309

Sen Zhang − Department of Chemistry, University of Virginia, Charlottesville, Virginia 22904, United States; orcid.org/0000-0002-1716-3741

Notes

The authors declare no competing financial interest.

Acknowledgments

The Gunnoe group acknowledges support from the U.S. National Science Foundation (1800173).

References

1. Godula, K.; Sames, D., C-H Bond Functionalization in Complex Organic Synthesis. *Science* **2006,** *312*, 67.

2. Gunnoe, T. B., Metal-Mediated Carbon–Hydrogen Bond Activation. In *Physical Inorganic Chemistry: Reactions, Processes, and Applications*, Bakac, A., Ed. Wiley-VCH: Weinheim, Germany, 2010; pp 495-549.

3. Webb, J. R.; Burgess, S. A.; Cundari, T. R.; Gunnoe, T. B., Activation of Carbon–hydrogen Bonds and Dihydrogen by 1,2-CH-addition Across Metal–heteroatom Bonds. *Dalton Trans.* **2013,** *42*, 16646-16665.

4. McKeown, B. A.; Habgood, L. G.; Cundari, T. R.; Gunnoe, T. B., Alkylation of Arenes Without Chelation Assistance: Transition Metal Catalysts with d^6 Electron Configurations. In *Catalytic Hydroarylation of Carbon-Carbon Multiple Bonds*, Ackermann, L., Ed. Wiley-VCH: Weinheim, Germany, 2017; pp 83-106.

5. Webb, J. R.; Bolaño, T.; Gunnoe, T. B., Catalytic Oxy-Functionalization of Methane and Other Hydrocarbons: Fundamental Advancements and New Strategies. *ChemSusChem* **2011,** *4*, 37-49.

6. Foley, N. A.; Lee, J. P.; Ke, Z.; Gunnoe, T. B.; Cundari, T. R., Ru(II) Catalysts Supported by Hydridotris(pyrazolyl)borate for the Hydroarylation of Olefins: Reaction Scope, Mechanistic Studies, and Guides for the Development of Improved Catalysts. *Acc. Chem. Res.* **2009,** *42*, 585-597.

7. Andreatta, J. R.; McKeown, B. A.; Gunnoe, T. B., Transition Metal Catalyzed Hydroarylation of Olefins Using Unactivated Substrates: Recent Developments and Challenges. *J. Organomet. Chem.* **2011,** *696*, 305-315.

8. Hartwig, J. F.; Larsen, M. A., Undirected, Homogeneous C–H Bond Functionalization: Challenges and Opportunities. *ACS Cent. Sci.* **2016,** *2*, 281-292.

9. Hartwig, J. F., Evolution of C–H Bond Functionalization from Methane to Methodology. *J. Am. Chem. Soc.* **2016,** *138*, 2-24.

10. Goldberg, K. I.; Goldman, A. S., Large-Scale Selective Functionalization of Alkanes. *Acc. Chem. Res.* **2017,** *50*, 620-626.

11. Gunsalus, N. J.; Koppaka, A.; Park, S. H.; Bischof, S. M.; Hashiguchi, B. G.; Periana, R. A., Homogeneous Functionalization of Methane. *Chem. Rev.* **2017,** *117*, 8521-8573.

12. Ackermann, L.; Habgood, L. G.; Gunnoe, T. B., *Catalytic hydroarylation of carbon-carbon multiple bonds*. Wiley-VCH: Wiesbaden, Germany, 2018.

13. Ackermann, L., Carboxylate-Assisted Transition-Metal-Catalyzed C−H Bond Functionalizations: Mechanism and Scope. *Chem. Rev.* **2011,** *111*, 1315-1345.

14. Goldman, A. S.; Goldberg, K. I., Organometallic C—H Bond Activation: An Introduction. In *Activation and Functionalization of C—H Bonds*, American Chemical Society: 2004; Vol. 885, pp 1-43.

15. Jones, W. D.; Feher, F. J., Comparative reactivities of hydrocarbon carbon-hydrogen bonds with a transition-metal complex. *Acc. Chem. Res.* **1989,** *22*, 91-100.

16. Xie, J.; Pan, C.; Abdukader, A.; Zhu, C., Gold-catalyzed C(sp3)–H bond functionalization. *Chem. Soc. Rev.* **2014,** *43*, 5245-5256.

17. Hashiguchi, B. G.; Bischof, S. M.; Konnick, M. M.; Periana, R. A., Designing Catalysts for Functionalization of Unactivated C–H Bonds Based on the CH Activation Reaction. *Acc. Chem. Res.* **2012,** *45*, 885-898.

18. Kozhushkov, S. I.; Ackermann, L., Ruthenium-catalyzed direct oxidative alkenylation of arenes through twofold C–H bond functionalization. *Chem. Sci.* **2013,** *4*, 886-896.

19. Gensch, T.; Hopkinson, M. N.; Glorius, F.; Wencel-Delord, J., Mild metal-catalyzed C–H activation: examples and concepts. *Chem. Soc. Rev.* **2016,** *45*, 2900-2936.

20. Mkhalid, I. A. I.; Barnard, J. H.; Marder, T. B.; Murphy, J. M.; Hartwig, J. F., C−H Activation for the Construction of C−B Bonds. *Chem. Rev.* **2010,** *110*, 890-931.

21. Murakami, K.; Yamada, S.; Kaneda, T.; Itami, K., C–H Functionalization of Azines. *Chem. Rev.* **2017,** *117*, 9302-9332.

22. Lyons, T. W.; Sanford, M. S., Palladium-Catalyzed Ligand-Directed C−H Functionalization Reactions. *Chem. Rev.* **2010,** *110*, 1147-1169.

23. Roudesly, F.; Oble, J.; Poli, G., Metal-catalyzed CH Activation/functionalization: The Fundamentals. *J. Mol. Catal. A: Chem.* **2017,** *426*, 275-296.

24. Xue, X.-S.; Ji, P.; Zhou, B.; Cheng, J.-P., The Essential Role of Bond Energetics in C–H Activation/Functionalization. *Chem. Rev.* **2017,** *117*, 8622-8648.

25. Hartwig, J. F., Catalytic C–H Functionalization. In *Organotransition metal chemistry: from bonding to catalysis*, University Science Books, U.S.: Sausalito, 2010; pp 825-876.

26. Kunin, A. J.; Eisenberg, R., Photochemical Carbonylation of Benzene by Iridium(I) and Rhodium(I) Square-planar Complexes. *Organometallics* **1988,** *7*, 2124-2129.

27. Periana, R. A.; Taube, D. J.; Gamble, S.; Taube, H.; Satoh, T.; Fujii, H., Platinum Catalysts for the High-Yield Oxidation of Methane to a Methanol Derivative. *Science* **1998,** *280*, 560-564.

28. Lin, M.; Shen, C.; Garcia-Zayas, E. A.; Sen, A., Catalytic Shilov Chemistry: Platinum Chloride-Catalyzed Oxidation of Terminal Methyl Groups by Dioxygen. *J. Am. Chem. Soc.* **2001,** *123*, 1000-1001.

29. Labinger, J. A.; Bercaw, J. E., Understanding and Exploiting C–H Bond Activation. *Nature* **2002,** *417*, 507.

30. Hartwig, J. F., Catalytic, Thermal, Regioselective Functionalization of Alkanes and Arenes with Borane Reagents. In *Activation and Functionalization of C—H Bonds*, American Chemical Society: 2004; Vol. 885, pp 136-154.

31. Ravi, M.; Ranocchiari, M.; van Bokhoven, J. A., The Direct Catalytic Oxidation of Methane to Methanol—A Critical Assessment. *Angew. Chem., Int. Ed.* **2017,** *56*, 16464-16483.

32. Goldshleger, N.; Tyabin, M.; Shilov, A.; Shteinman, A., Activation of Saturated Hydrocarbons-deuterium-hydrogen Exchange in Solutions of Transition Metal Complexes. *Russ. J. Phys. Chem.* **1969,** *43*, 1222-1223.

33. Choi, J.; MacArthur, A. H. R.; Brookhart, M.; Goldman, A. S., Dehydrogenation and Related Reactions Catalyzed by Iridium Pincer Complexes. *Chem. Rev.* **2011,** *111*, 1761-1779.

34. Kumar, A.; Bhatti, T. M.; Goldman, A. S., Dehydrogenation of Alkanes and Aliphatic Groups by Pincer-Ligated Metal Complexes. *Chem. Rev.* **2017,** *117*, 12357-12384.

35. Shilov, A. E.; Shul'pin, G. B., Activation of C−H Bonds by Metal Complexes. *Chem. Rev.* **1997,** *97*, 2879-2932.

36. Wedi, P.; van Gemmeren, M., Arene-Limited Nondirected C−H Activation of Arenes. *Angew. Chem., Int. Ed.* **2018,** *57*, 13016-13027.

37. Schranck, J.; Tlili, A.; Beller, M., Functionalization of Remote C-H Bonds: Expanding the Frontier. *Angew. Chem., Int. Ed.* **2014,** *53*, 9426-9428.

38. Haibach, M. C.; Kundu, S.; Brookhart, M.; Goldman, A. S., Alkane Metathesis by Tandem Alkane-Dehydrogenation–Olefin-Metathesis Catalysis and Related Chemistry. *Acc. Chem. Res.* **2012,** *45*, 947-958.

39. Prendergast, A. M.; McGlacken, G. P., Transition Metal Mediated C–H Activation of 2-Pyrones, 2-Pyridones, 2-Coumarins and 2-Quinolones. *Eur. J. Org. Chem.* **2018,** *2018*, 6068-6082.

40. Brandhofer, T.; García Mancheño, O., Site-Selective C–H Bond Activation/Functionalization of Alpha-Amino Acids and Peptide-Like Derivatives. *Eur. J. Org. Chem.* **2018,** *2018*, 6050-6067.

41. Jun, C. H.; Lee, J. H., Application of C-H and C-C bond activation in organic synthesis. *Pure Appl. Chem.* **2004,** *76*, 577-587.

42. Periana, R. A.; Bhalla, G.; Tenn, W. J.; Young, K. J. H.; Liu, X. Y.; Mironov, O.; Jones, C. J.; Ziatdinov, V. R., Perspectives on Some Challenges and Approaches for Developing the Next Generation of Selective, Low Temperature, Oxidation Catalysts for Alkane Hydroxylation Based on the CH Activation Reaction. *J. Mol. Catal. A: Chem.* **2004,** *220*, 7-25.

43. Whisler, M. C.; MacNeil, S.; Snieckus, V.; Beak, P., Beyond Thermodynamic Acidity: A Perspective on the Complex-Induced Proximity Effect (CIPE) in Deprotonation Reactions. *Angew. Chem., Int. Ed.* **2004,** *43*, 2206-2225.

44. Sambiagio, C.; Schönbauer, D.; Blieck, R.; Dao-Huy, T.; Pototschnig, G.; Schaaf, P.; Wiesinger, T.; Zia, M. F.; Wencel-Delord, J.; Besset, T.; Maes, B. U. W.; Schnürch, M., A comprehensive overview of directing groups applied in metal-catalysed C–H functionalisation chemistry. *Chem. Soc. Rev.* **2018,** *47*, 6603-6743.

45. St John-Campbell, S.; Bull, J. A., Transient imines as 'next generation' directing groups for the catalytic functionalisation of C–H bonds in a single operation. *Org. Biomol. Chem.* **2018,** *16*, 4582-4595.

46. Gandeepan, P.; Ackermann, L., Transient Directing Groups for Transformative C–H Activation by Synergistic Metal Catalysis. *Chem* **2018,** *4*, 199-222.

47. Dey, A.; Agasti, S.; Maiti, D., Palladium catalysed meta-C–H functionalization reactions. *Org. Biomol. Chem.* **2016,** *14*, 5440-5453.

48. Rouquet, G.; Chatani, N., Catalytic Functionalization of C(sp2)-H and C(sp3)-H Bonds by Using Bidentate Directing Groups. *Angew. Chem., Int. Ed.* **2013,** *52*, 11726-11743.

49. Engle, K. M.; Mei, T.-S.; Wasa, M.; Yu, J.-Q., Weak Coordination as a Powerful Means for Developing Broadly Useful C–H Functionalization Reactions. *Acc. Chem. Res.* **2012,** *45*, 788-802.

50. Colby, D. A.; Bergman, R. G.; Ellman, J. A., Rhodium-Catalyzed C−C Bond Formation via Heteroatom-Directed C−H Bond Activation. *Chem. Rev.* **2010,** *110*, 624-655.

51. Ackermann, L.; Vicente, R.; Althammer, A., Assisted Ruthenium-Catalyzed C−H Bond Activation: Carboxylic Acids as Cocatalysts for Generally Applicable Direct Arylations in Apolar Solvents. *Org. Lett.* **2008,** *10*, 2299-2302.

52. Ahlquist, M.; Periana, R. A.; Goddard, W. A., C–H Activation in Strongly Acidic Media. The Co-catalytic Effect of the Reaction Medium. *Chem. Commun.* **2009**, 2373-2375.

53. Gao, X.-A.; Yan, R.-L.; Wang, X.-X.; Yan, H.; Li, J.; Guo, H.; Huang, G.-S., Pd(II)-Catalyzed Synthesis of Benzisoxazolones from Benzohydroxamic Acids via C–H Activation. *J. Org. Chem.* **2012,** *77*, 7700-7705.

54. Athira, C.; Sunoj, R. B., Role of Lewis acid additives in a palladium catalyzed directed C-H functionalization reaction of benzohydroxamic acid to isoxazolone. *Org. Biomol. Chem.* **2017,** *15*, 246-255.

55. Tischler, O.; Bokányi, Z.; Novák, Z., Activation of C–H Activation: The Beneficial Effect of Catalytic Amount of Triaryl Boranes on Palladium-Catalyzed C–H Activation. *Organometallics* **2016,** *35*, 741-746.

56. Váňa, J.; Terencio, T.; Petrović, V.; Tischler, O.; Novák, Z.; Roithová, J., Palladium-Catalyzed C–H Activation: Mass Spectrometric Approach to Reaction Kinetics in Solution. *Organometallics* **2017,** *36*, 2072-2080.

57. Tischler, O.; Kovács, S.; Érsek, G.; Králl, P.; Daru, J.; Stirling, A.; Novák, Z., Study of Lewis Acid Accelerated Palladium Catalyzed CH Activation. *J. Mol. Catal. A: Chem.* **2017,** *426*, 444-450.

58. Gao, Y.; Guan, C.; Zhou, M.; Kumar, A.; Emge, T. J.; Wright, A. M.; Goldberg, K. I.; Krogh-Jespersen, K.; Goldman, A. S., β-Hydride Elimination and C–H Activation by an Iridium Acetate Complex, Catalyzed by Lewis Acids. Alkane Dehydrogenation Cocatalyzed by Lewis Acids and [2,6-Bis(4,4-dimethyloxazolinyl)-3,5-dimethylphenyl]iridium. *J. Am. Chem. Soc.* **2017,** *139*, 6338-6350.

59. Zhu, W.; Luo, Z.; Chen, J.; Liu, C.; Yang, L.; Dickie, D. A.; Liu, N.; Zhang, S.; Davis, R. J.; Gunnoe, T. B., Mechanistic Studies of Single-Step Styrene Production Catalyzed by Rh Complexes with Diimine Ligands: An Evaluation of the Role of Ligands and Induction Period. *ACS Catal.* **2019,** *9*, 7457-7475.

60. Liebov, N. S.; Zhu, W.; Chen, J.; Webster-Gardiner, M. S.; Schinski, W. L.; Gunnoe, T. B., Rhodium-Catalyzed Alkenylation of Toluene Using 1-Pentene: Regioselectivity To Generate Precursors for Bicyclic Compounds. *Organometallics* **2019,** *38*, 3860-3870.

61. Chen, J.; Nielsen, R. J.; Goddard, W. A.; McKeown, B. A.; Dickie, D. A.; Gunnoe, T. B., Catalytic Synthesis of Superlinear Alkenyl Arenes Using a Rh(I) Catalyst Supported by a "Capping Arene" Ligand: Access to Aerobic Catalysis. *J. Am. Chem. Soc.* **2018,** *140*, 17007-17018.

62. Webster-Gardiner, M. S.; Chen, J.; Vaughan, B. A.; McKeown, B. A.; Schinski, W.; Gunnoe, T. B., Catalytic Synthesis of "Super" Linear Alkenyl Arenes Using an Easily Prepared Rh(I) Catalyst. *J. Am. Chem. Soc.* **2017,** *139*, 5474-5480.

63. Vaughan, B. A.; Khani, S. K.; Gary, J. B.; Kammert, J. D.; Webster-Gardiner, M. S.; McKeown, B. A.; Davis, R. J.; Cundari, T. R.; Gunnoe, T. B., Mechanistic Studies of Single-Step Styrene Production Using a Rhodium(I) Catalyst. *J. Am. Chem. Soc.* **2017,** *139*, 1485-1498.

64. Webster-Gardiner, M. S.; Fu, R.; Fortman, G. C.; Nielsen, R. J.; Gunnoe, T. B.; Goddard, W. A., Arene C–H Activation Using Rh(i) Catalysts Supported by Bidentate Nitrogen Chelates. *Catal. Sci. Technol.* **2015,** *5*, 96-100.

65. Vaughan, B. A.; Webster-Gardiner, M. S.; Cundari, T. R.; Gunnoe, T. B., A Rhodium Catalyst for Single-step Styrene Production from Benzene and Ethylene. *Science* **2015,** *348*, 421-424.

66. Fu, R.; O'Reilly, M. E.; Nielsen, R. J.; Goddard Iii , W. A.; Gunnoe, T. B., Rhodium Bis(quinolinyl)benzene Complexes for Methane Activation and Functionalization. *Chem. Eur. J.* **2015,** *21*, 1286-1293.

67. Zhu, W.; Gunnoe, T. B., Advances in Rhodium-Catalyzed Oxidative Arene Alkenylation. *Acc. Chem. Res.* **2020,** *53*, 920-936.

68. O'Reilly, M. E.; Fu, R.; Nielsen, R. J.; Sabat, M.; Goddard, W. A.; Gunnoe, T. B., Long-Range C–H Bond Activation by RhIII-Carboxylates. *J. Am. Chem. Soc.* **2014,** *136*, 14690-14693.

69. Jia, X.; Frye, L. I.; Zhu, W.; Gu, S.; Gunnoe, T. B., Synthesis of Stilbenes by Rhodium-Catalyzed Aerobic Alkenylation of Arenes via C–H Activation. *J. Am. Chem. Soc.* **2020,** *142*, 10534-10543.

70. Atzrodt, J.; Derdau, V.; Fey, T.; Zimmermann, J., The Renaissance of H/D Exchange. *Angew. Chem., Int. Ed.* **2007,** *46*, 7744-7765.

71. Junk, T.; Catallo, W. J., Hydrogen Isotope Exchange Reactions Involving C–H (D, T) Bonds. *Chem. Soc. Rev.* **1997,** *26*, 401-406.

72. Jones, W. D., Isotope Effects in C−H Bond Activation Reactions by Transition Metals. *Acc. Chem. Res.* **2003,** *36*, 140-146.

73. Burwell, R. L., Deuterium as a Tracer in Reactions of Hydrocarbons on Metallic Catalysts. *Acc. Chem. Res.* **1969,** *2*, 289-296.

74. Lockley, W. J. S.; Heys, J. R., Metal-catalysed Hydrogen Isotope Exchange Labelling: A Brief Overview. *J. Labelled Compd. Radiopharm.* **2010,** *53*, 635-644.

75. Lersch, M.; Tilset, M., Mechanistic Aspects of C−H Activation by Pt Complexes. *Chem. Rev.* **2005,** *105*, 2471-2526.

76. Rhinehart, J. L.; Manbeck, K. A.; Buzak, S. K.; Lippa, G. M.; Brennessel, W. W.; Goldberg, K. I.; Jones, W. D., Catalytic Arene H/D Exchange with Novel Rhodium and Iridium Complexes. *Organometallics* **2012,** *31*, 1943-1952.

77. Feng, Y.; Jiang, B.; Boyle, P. A.; Ison, E. A., Effect of Ancillary Ligands and Solvents on H/D Exchange Reactions Catalyzed by Cp*Ir Complexes. *Organometallics* **2010,** *29*, 2857-2867.

78. Hickman, A. J.; Villalobos, J. M.; Sanford, M. S., Quantitative Assay for the Direct Comparison of Platinum Catalysts in Benzene H/D Exchange. *Organometallics* **2009,** *28*, 5316-5322.

79. Munz, D.; Webster-Gardiner, M.; Fu, R.; Strassner, T.; Goddard, W. A.; Gunnoe, T. B., Proton or Metal? The H/D Exchange of Arenes in Acidic Solvents. *ACS Catal.* **2015,** *5*, 769-775.

80. Webster-Gardiner, M. S.; Piszel, P. E.; Fu, R.; McKeown, B. A.; Nielsen, R. J.; Goddard, W. A.; Gunnoe, T. B., Electrophilic RhI Catalysts for Arene H/D Exchange in Acidic Media: Evidence for an Electrophilic Aromatic Substitution Mechanism. *J. Mol. Catal. A: Chem.* **2017,** *426*, 381-388.

81. Feller, M.; Diskin-Posner, Y.; Leitus, G.; Shimon, L. J. W.; Milstein, D., Direct Observation of Reductive Elimination of MeX (X = Cl, Br, I) from RhIII Complexes: Mechanistic Insight and the Importance of Sterics. *J. Am. Chem. Soc.* **2013,** *135*, 11040-11047.

82. Feller, M.; Iron, M. A.; Shimon, L. J. W.; Diskin-Posner, Y.; Leitus, G.; Milstein, D., Competitive C−I versus C−CN Reductive Elimination from a RhIII Complex. Selectivity is Controlled by the Solvent. *J. Am. Chem. Soc.* **2008,** *130*, 14374-14375.

83. Gu, S.; Nielsen, R. J.; Taylor, K. H.; Fortman, G. C.; Chen, J.; Dickie, D. A.; Goddard, W. A.; Gunnoe, T. B., Use of Ligand Steric Properties to Control the Thermodynamics and Kinetics of Oxidative Addition and Reductive Elimination with Pincer-Ligated Rh Complexes. *Organometallics* **2020,** *39*, 1917-1933.

84. Hanson, S. K.; Heinekey, D. M.; Goldberg, K. I., C−H Bond Activation by Rhodium(I) Phenoxide and Acetate Complexes: Mechanism of H−D Exchange between Arenes and Water. *Organometallics* **2008,** *27*, 1454-1463.

85. Gair, J. J.; Qiu, Y.; Chan, N. H.; Filatov, A. S.; Lewis, J. C., Rhodium Complexes of 2,6-Bis(dialkylphosphinomethyl)pyridines: Improved C–H Activation, Expanded Reaction Scope, and Catalytic Direct Arylation. *Organometallics* **2017,** *36*, 4699-4706.

86. Christine, H.; Michael, S.; Eberhardt, H.; Rudolf, T., Synthesis and Characterization of Organorhodium(I) Complexes with the Tridentate Ligand 2,6-Bis(diphenylphosphanylmethyl)pyridine [Rh(PNP)R] (R = CH3, C6H5) and Their Reactivity toward Ethylene and Protic Acids. *Eur. J. Inorg. Chem.* **1998,** *1998*, 1425-1432.

87. Feller, M.; Ben-Ari, E.; Gupta, T.; Shimon, L. J. W.; Leitus, G.; Diskin-Posner, Y.; Weiner, L.; Milstein, D., Mononuclear Rh(II) PNP-Type Complexes. Structure and Reactivity. *Inorg. Chem.* **2007,** *46*, 10479-10490.

88. Jia, X.; Foley, A. M.; Liu, C.; Vaughan, B. A.; McKeown, B. A.; Zhang, S.; Gunnoe, T. B., Styrene Production from Benzene and Ethylene Catalyzed by Palladium(II): Enhancement of Selectivity toward Styrene via Temperature-dependent Vinyl Ester Consumption. *Organometallics* **2019,** *38*, 3532-3541.

89. Prechtl, M. H. G.; Hölscher, M.; Ben-David, Y.; Theyssen, N.; Loschen, R.; Milstein, D.; Leitner, W., H/D Exchange at Aromatic and Heteroaromatic Hydrocarbons Using D2O as the Deuterium Source and Ruthenium Dihydrogen Complexes as the Catalyst. *Angew. Chem., Int. Ed.* **2007,** *46*, 2269-2272.

90. Lockley, W. J. S.; Hesk, D., Rhodium- and ruthenium-catalysed hydrogen isotope exchange. *J. Labelled Compd. Radiopharm.* **2010,** *53*, 704-715.

91. Iluc, V. M.; Fedorov, A.; Grubbs, R. H., H/D Exchange Processes Catalyzed by an Iridium-Pincer Complex. *Organometallics* **2012,** *31*, 39-41.

92. Jones, W. D.; Feher, F. J., Mechanism of arene carbon-hydrogen bond activation by (C5Me5)Rh(PMe3)(H)Ph. Evidence for arene precoordination. *J. Am. Chem. Soc.* **1982,** *104*, 4240-4242.

93. Toledo, I.; Arancibia, M.; Andrade, C.; Crivelli, I., Redox chemistry of copper acetate binuclear complexes in acetic acid-methanol mixture as solvent. *Polyhedron* **1998,** *17*, 173-178.

94. Sperotto, E.; van Klink, G. P. M.; van Koten, G.; de Vries, J. G., The mechanism of the modified Ullmann reaction. *Dalton Trans.* **2010,** *39*, 10338-10351.

95. Zabawa, T. P.; Kasi, D.; Chemler, S. R., Copper(II) Acetate Promoted Intramolecular Diamination of Unactivated Olefins. *J. Am. Chem. Soc.* **2005,** *127*, 11250-11251.

96. Johansson, L.; Ryan, O. B.; Rømming, C.; Tilset, M., Unexpected Selectivities in C−H Activations of Toluene and p-Xylene at Cationic Platinum(II) Diimine Complexes. New Mechanistic Insight into Product-Determining Factors. *J. Am. Chem. Soc.* **2001,** *123*, 6579-6590.

97. Shanahan, J. P.; Szymczak, N. K., Lewis Acid Effects on Calculated Ligand Electronic Parameters. *Organometallics* **2020** ASAP.

98. Kloek, S. M.; Heinekey, D. M.; Goldberg, K. I., C−H Bond Activation by Rhodium(I) Hydroxide and Phenoxide Complexes. *Angew. Chem., Int. Ed.* **2007,** *46*, 4736-4738.

99. Christine, H.; Michael, S.; Eberhardt, H.; Rudolf, T., Oxidative Addition Reactions of Organorhodium(I) Complexes Containing the Tridentate Ligand 2,6-Bis(diphenylphosphanylmethyl)pyridine [Rh(PNP)R] (R = CH3, C6H5) with Iodine and Methyl Iodide and Investigation of the Reductive Elimination. *Eur. J. Inorg. Chem.* **1999,** *1999*, 435-440.

100. Davies, D. L.; Macgregor, S. A.; McMullin, C. L., Computational Studies of Carboxylate-Assisted C–H Activation and Functionalization at Group 8–10 Transition Metal Centers. *Chem. Rev.* **2017,** *117*, 8649-8709.

101. Lapointe, D.; Fagnou, K., Overview of the Mechanistic Work on the Concerted Metallation–Deprotonation Pathway. *Chem. Lett.* **2010,** *39*, 1118-1126.

102. Yuan, H.; Brennessel, W. W.; Jones, W. D., Effect of Carboxylate Ligands on Alkane Dehydrogenation with (dmPhebox)Ir Complexes. *ACS Catal.* **2018,** *8*, 2326-2329.

103. Boyd, E. A.; Lionetti, D.; Henke, W. C.; Day, V. W.; Blakemore, J. D., Preparation, Characterization, and Electrochemical Activation of a Model [Cp*Rh] Hydride. *Inorg. Chem.* **2019,** *58*, 3606-3615.

104. Gair, J. J.; Qiu, Y.; Khade, R. L.; Chan, N. H.; Filatov, A. S.; Zhang, Y.; Lewis, J. C., Synthesis, Characterization, and Theoretical Investigation of a Transition State Analogue for Proton Transfer during C–H Activation by a Rhodium-Pincer Complex. *Organometallics* **2019,** *38*, 1407-1412.

105. Anaby, A.; Feller, M.; Ben-David, Y.; Leitus, G.; Diskin-Posner, Y.; Shimon, L. J. W.; Milstein, D., Bottom-Up Construction of a CO_2-Based Cycle for the Photocarbonylation of Benzene, Promoted by a Rhodium(I) Pincer Complex. *J. Am. Chem. Soc.* **2016,** *138*, 9941-9950.

106. Feller, M.; Diskin-Posner, Y.; Shimon, L. J. W.; Ben-Ari, E.; Milstein, D., N–H Activation by Rh(I) via Metal–Ligand Cooperation. *Organometallics* **2012,** *31*, 4083-4101.

107. Frech, C. M.; Milstein, D., Direct Observation of Reductive Elimination of Methyl Iodide from a Rhodium(III) Pincer Complex: The Importance of Sterics. *J. Am. Chem. Soc.* **2006,** *128*, 12434-12435.

108. Beck, C. M.; Rathmill, S. E.; Park, Y. J.; Chen, J.; Crabtree, R. H.; Liable-Sands, L. M.; Rheingold, A. L., Aldehyde Decarbonylation Catalysis under Mild Conditions. *Organometallics* **1999,** *18*, 5311-5317.

109. Doughty, D. H.; Pignolet, L. H., Catalytic decarbonylation of aldehydes. *J. Am. Chem. Soc.* **1978,** *100*, 7083-7085.

110. Tsuji, J.; Ohno, K., Organic syntheses by means of noble metal compounds XXI. Decarbonylation of aldehydes using rhodium complex. *Tetrahedron Lett.* **1965,** *6*, 3969-3971.

111. Abu-Hasanayn, F.; Goldman, M. E.; Goldman, A. S., Development and mechanistic study of a new aldehyde decarbonylation catalyst. *J. Am. Chem. Soc.* **1992,** *114*, 2520-2524.

112. O'Connor, J. M.; Ma, J., A high-yield conversion of trans-carbonylchlorobis(triphenylphosphine)rhodium to chlorotris(triphenylphosphine) rhodium. *Inorg. Chem.* **1993,** *32*, 1866-1867.

113. Sun, Z.-M.; Zhang, J.; Zhao, P., Rh(I)-Catalyzed Decarboxylative Transformations of Arenecarboxylic Acids: Ligand- and Reagent-Controlled Selectivity toward Hydrodecarboxylation or Heck−Mizoroki Products. *Org. Lett.* **2010,** *12*, 992-995.

114. Sun, Z.-M.; Zhao, P., Rhodium-Mediated Decarboxylative Conjugate Addition of Fluorinated Benzoic Acids: Stoichiometric and Catalytic Transformations. *Angew. Chem., Int. Ed.* **2009,** *48*, 6726-6730.

115. Fulmer, G. R.; Miller, A. J. M.; Sherden, N. H.; Gottlieb, H. E.; Nudelman, A.; Stoltz, B. M.; Bercaw, J. E.; Goldberg, K. I., NMR Chemical Shifts of Trace Impurities: Common Laboratory Solvents, Organics, and Gases in Deuterated Solvents Relevant to the Organometallic Chemist. *Organometallics* **2010,** *29*, 2176-2179.

Table of Contents Graphic